



University of Glasgow
DEPARTMENT OF
**AEROSPACE
ENGINEERING**

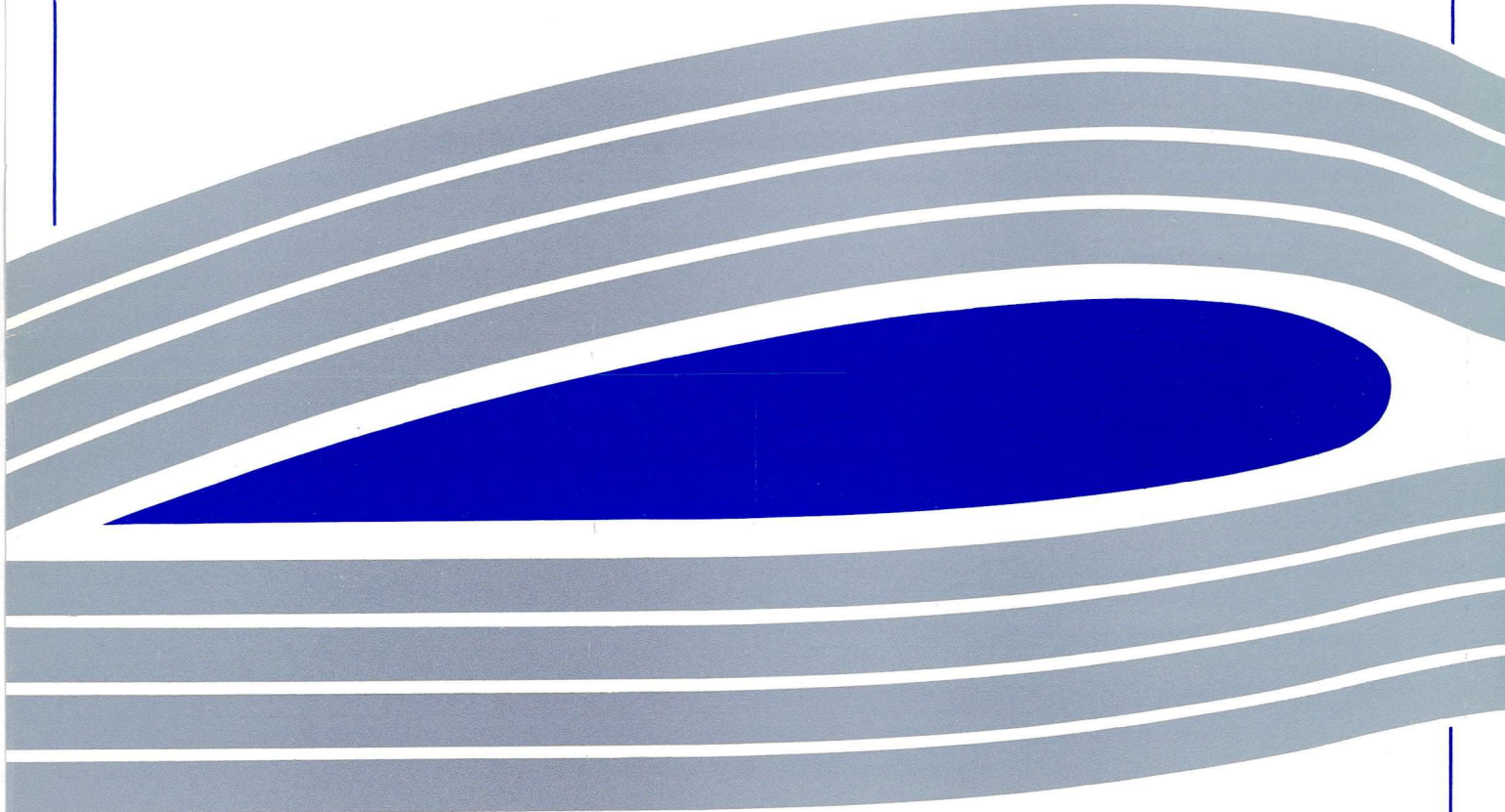


Engineering
PERIODICALS

U7000

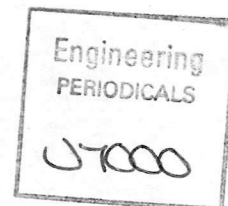
**Helicopter Takeoff and Landing Procedures
In Adverse Conditions Using Inverse Simulation**

Progress Note : Oct. 92 - Sept. 93



Internal Report No. 9332

University Agreement No. 7D/S/960



**Helicopter Takeoff and Landing Procedures
In Adverse Conditions Using Inverse Simulation**

Progress Note : Oct. 92 - Sept. 93

by

C. Taylor, D.G. Thomson, R. Bradley

Department of Aerospace Engineering - University of Glasgow

Summary

This report summarises the progress made in the second year of a study of helicopter offshore operations in adverse conditions. Initially, a narrative description of key helicopter heli-deck related manoeuvres in the presence and absence of engine failures, is given. Based on this information, mathematical models of the manoeuvres are developed in a form suitable for use as input to inverse simulation. The demands of simulating pilot strategies in the event of engine failures has necessitated the development of a multistage inverse-forward-inverse simulation technique of novel kind and a comprehensive description of this method is presented. A dynamic graphics package has been created to demonstrate piloting strategies and its formulation is briefly outlined. The piloting strategies as derived from simulation studies are presented for the Towering Takeoff and Normal Approach and Landing manoeuvres (with and without engine failures) and these are qualitatively validated against descriptions provided by practicing pilots. Finally, some conclusions are drawn and directions for future work highlighted.

Contents

- 1. Introduction**
- 2. A Pilots View of Helicopter Off shore Manoeuvres**
 - 2.1 The Towering Takeoff Manoeuvre
 - 2.2 Piloting Aspects of Flying
 - 2.3 The Piloting Strategy for a Towering Takeoff
 - 2.4 Piloting Strategy for Recovery from Engine Failure During a Towering Takeoff
 - 2.5 The Normal Approach and Landing Manoeuvre
 - 2.6 Piloting Aspects of the Normal Approach and Landing Manoeuvre
 - 2.7 A Possible Strategy for the Normal Approach and Landing
 - 2.8 A Possible Strategy for the Approach and Landing With an Engine Failure
- 3. Mathematical Representation of Offshore Flight Paths**
 - 3.1 A Mathematical Description of the Towering Takeoff Manoeuvre
 - 3.2 A Mathematical Description of the Normal Approach and Landing Manoeuvre
- 4. Modelling Developments**
 - 4.1 Twin Engine Model
 - 4.2 Artificial Stability and Flight Control System
- 5. Simulation Developments**
 - 5.1 Inverse - Forward - Inverse Simulation
 - 5.2 Development of Blending Functions
- 6. Helicopter Offshore Graphical Simulation**
- 7. Qualitative Validation and Analysis of Results**
 - 7.1 Inverse Simulation of the Towering Takeoff Manoeuvre
 - 7.2 Inverse Simulation of Engine Failures During Towering Takeoff
 - 7.3 Inverse Simulation of Normal Approach and Landing
 - 7.4 Inverse Simulation of Engine Failures During Normal Approach and Landing Manoeuvres
- 8. Conclusions**

Acknowledgements

References

Appendix 1

Appendix 2

Figures

Nomenclature

| | | |
|--------------------------------|---|---------------------|
| a_z | Vertical acceleration in helicopter body axes | (m/s ²) |
| g | Acceleration due to gravity | (m/s ²) |
| h_{FLR} | Flare height | (m) |
| h_{LDP} | Landing decision point height | (m) |
| h_{TDP} | Takeoff decision point height | (m) |
| K_{e1} | Gains associated with change in rotor speed | (kg/rad) |
| K_{e2} | Gains associated with change in engine torque | (Nms/kg) |
| K_3 | Overall gain of engine governing system | (Nms/rad) |
| Q_E | Engine torque | (Nm) |
| $Q_{E\ IDLE}$ | Engine torque at flight idle | (Nm) |
| $Q_{E\ LIM}$ | Maximum single engine torque output | (Nm) |
| $Q_{E\ MAX}$ | Total maximum allowable engine torque | (Nm) |
| Q_R | Main rotor torque | (Nm) |
| Q_{TR} | Tail rotor torque | (Nm) |
| N_R | Rotor speed | |
| s | Laplace operator | |
| t | Flight time | (s) |
| t_{CP} | Time for collective pulse | (s) |
| t_{FLR} | Flare time | (s) |
| t_{LDP} | Landing decision point time | (s) |
| t_m | Manoeuvre time | (s) |
| t_{TDP} | Takeoff decision point time | (s) |
| v_{TDP} | Rate of climb at takeoff decision point | (m/s) |
| v_{tm} | Descent rate on manoeuvre exit | (m/s) |
| V_{BLSS} | Baulked landing safety speed | (m/s) |
| V_E | Manoeuvre exit velocity | (m/s) |
| V_{LDP} | Landing decision point flight velocity | (m/s) |
| \dot{V}_{max} | Peak longitudinal flight path acceleration | (m/s ²) |
| w_f | Fuel flow | (kg/s) |
| $w_{f\ IDLE}$ | Fuel flow at flight idle | (kg/s) |
| x, y, z | Component of flight path co-ordinates | (m) |
| $\dot{x}, \dot{y}, \dot{z}$ | Components of translational velocities | (m/s) |
| $\ddot{x}, \ddot{y}, \ddot{z}$ | Components of translational accelerations | (m/s ²) |
| \ddot{x}_{max} | Maximum longitudinal acceleration | (m/s ²) |
| \ddot{x}_{min} | Minimum longitudinal acceleration | (m/s ²) |

Greek Symbols

| | | |
|--|--|-----------------------|
| γ | Flight path angle | (rad) |
| γ_E | Manoeuvre exit climb angle | (rad) |
| γ_{LDP} | Landing decision point descent angle | (rad) |
| γ_{MAX} | Maximum descent angle during approach | (rad) |
| δ | Recovery lag | |
| η_c | Pilot collective lever position | |
| η_{1s} | Longitudinal cyclic stick position | |
| η_{1c} | Lateral cyclic stick position | |
| η_p | Pedal position | |
| η_{ct} | Cable length | |
| θ, ϕ, ψ | Body attitude angles | (rad) |
| θ_o, θ_{ot} | Main and tailrotor collective blade pitch angles | (rad) |
| θ_{1s}, θ_{1c} | Cyclic blade pitch angles | (rad) |
| $\theta_{op}, \theta_{otp}$ | Pilot contribution to main and tailrotor collective angles | (rad) |
| $\theta_{1sp}, \theta_{1cp}$ | Pilot contribution to cyclic pitch | (rad) |
| $\theta_{oa}, \theta_{ota}$ | Autostab contribution to collective pitch angles | (rad) |
| $\theta_{1sa}, \theta_{1ca}$ | Autostab contribution to cyclic pitch | (rad) |
| $\tau_{e1}, \tau_{e2}, \tau_{e3}$ | Time constants associated with engine governor | (s) |
| $\tau_{c1}, \tau_{c2}, \tau_{c3}, \tau_{c4}$ | Time constants associated with flight control actuators | (s) |
| ψ_f | Cyclic mixing angle | (rad) |
| Ω | Angular velocity of rotor | (rad/s) |
| Ω_{IDLE} | Angular velocity of rotor at flight idle | (rad/s) |
| $\Omega_{Q_{MAX}}$ | Angular velocity of rotor at maximum engine torque | (rad/s) |
| $\dot{\Omega}$ | Angular acceleration of the rotor | (rad/s ²) |

Abbreviations

| | |
|------|--|
| AEO | All Engines Operating |
| BCAR | British Civil Airworthiness Requirements |
| CTO | Continued Takeoff |
| FAR | Federal Aviation Requirements |
| LDP | Landing Decision Point |
| OEI | One Engine Inoperative |
| TDP | Takeoff Decision Point |
| RTO | Rejected Takeoff |
| WAT | Weight and Temperature |

1. Introduction

This report documents the progress made during the second year of an inverse simulation investigation of helicopter offshore operations under adverse conditions. During this year, the work has built on the fundamental rotor inflow modelling enhancements implemented in the first twelve months of research, documented in an earlier report [1] and consequently the influence of ground effect, the vortex ring state and dynamic inflow were all incorporated. Furthermore, the availability of basic trajectory and pilot strategy data [2, 3, 4, 5] relating to manoeuvres commonly employed in offshore operations enabled preliminary simulation studies using the inverse simulation package, Helinv, to be performed. The basis of the inverse algorithm is its ability to calculate control displacements required for the modelled vehicle to fly a predetermined flight path, which in effect is the simulation input. Consequently, a range of offshore manoeuvres were modelled using smoothly connected polynomial functions of time to describe the principle manoeuvre parameters. These manoeuvres include the Towering Takeoff, Normal Approach and Landing and Aborted Approach. Initial simulation results proved encouraging and provided further credence to the inverse method as an appropriate tool with which to investigate offshore manoeuvres and pilot strategies.

The progress made in the first twelve months of research enabled the effort in the second year to concentrate on pilot strategies in the event of engine failures. Consequently, comprehensive descriptions of trajectories and pilot strategies were obtained for the Towering Takeoff and Normal Approach and Landing manoeuvres (with and without engine failures) and these are presented in section 2. This information, highlighted the salient features of these key offshore manoeuvres and enabled refinement of the original mathematical models of the flight paths. Furthermore a new approach of modelling the manoeuvres as a series of smooth pulses of acceleration was adopted. The details of the new method of modelling the flight paths and the flight paths themselves are outlined in section 3 of this report.

An important element of this years work has been the modification of the existing helicopter model to include a twin engine powerplant and an automatic stability and flight control system. The original version of Helinv employed a helicopter mathematical model [6] that modelled a single engine powerplant only. The development of a more realistic mathematical model of a twin engine, torque limited powerplant capable of accommodating multiple or single gas turbine failures is discussed in section 4.1 of this document. The control displacements evaluated in the original version of the inverse algorithm are presented in the form of swash-plate angles, whereas for this investigation results in the form of pilot collective lever, cyclic stick and pedal displacements are required. Thus a stability augmentation and flight control system has

been included into the mathematical model of the helicopter. The mathematical model of the stability augmentation and flight control system is of a type commonly found in conventional helicopter flight mechanic models and is discussed in section 4.2 of this progress report.

The need to take into account the pilot's reaction time in the event of an engine failure has also been addressed. Through careful application of conventional and inverse simulation methods, a novel hybrid simulation technique that incorporates both inverse and forward methods has been developed, enabling variations in pilot response time to be accommodated. The formulation of this algorithm and the subsequent specialised recovery trajectories required are detailed in section 5.

With the modelling and simulation developments mentioned above, large quantities of complex and detailed vehicle flight path, control and state vector information can be generated. Currently, with the absence of suitable flight test data, interpretation and verification of these results can be a demanding task. One tool that provides a useful and effective means of tackling this problem is the use of graphical presentation techniques. To this end, a computer simulated, three dimensional, helicopter offshore environment has been created on a Silicon Graphics Iris Indigo workstation. The software is known as Hogs (**H**elicopter **O**ffshore **G**raphical **S**imulation) and written in the 'C' programming language, and makes extensive use of the supporting graphic libraries available within the Iris computer. The graphical simulation package uses input data generated from the Helinv simulation package. Details of the Hogs software and its architecture is given in section 6 of this progress report.

Validation of results is an integral part of any simulation investigation. With no appropriate flight test data currently available, comparison of flight test and simulated results is clearly not possible. In section 7 of this report, qualitative validation of the analytical and simulation techniques has been achieved by the comparison of actual and simulated control strategies adopted for Towering Takeoff and Normal Approach and Landing manoeuvres. Detailed accounts of piloting strategy during takeoff and landing manoeuvres with an engine are also given.

2. A Pilots View of Helicopter Offshore Manoeuvres

2.1. The Towering Take-off Manoeuvre

The validity of the results from any inverse simulation will depend to a large degree on the accuracy of the manoeuvre description. For the current study careful consideration has been made of both piloting information and that contained in the regulatory bodies documents [5].

2.2 Piloting Aspects of Flying the Towering Take-off Manoeuvre

The Towering Take-off is commonly used during multi-engine helicopter offshore operations as an efficient means of departing from elevated helidecks, since the manoeuvre gives the best possibility of survival of an engine failure. An engine failure during this low speed phase of flight will quickly result in unacceptable loss of rotor RPM (Nr) unless prompt pilot action is taken to lower the collective and therefore reduce the power required to that available from the remaining good engine of a twin engine helicopter. This reduction of collective pitch results in a loss of height so the pilot has to ensure that the aircraft will either land back on the helideck below, or ensure sufficient forward motion that the flight path will clear the deck edge by a safe margin. This latter case can only be achieved when sufficient height has been gained and therefore there is a critical height above the helideck, known as the Take-off Decision Point (TDP), before which the take-off must be rejected and a landing carried out onto the helideck, and after which the take-off can be continued, possibly descending past and below the deck edge into forward flight.

The optimum technique for any given situation and type of helicopter is dependent on various factors :

- i) All-Engine Operating Power. There must be sufficient All-Engines Operating (AEO) power available to allow a vertical climb in the ambient conditions at the actual helicopter weight.
- ii) Single Engine Power. There must be sufficient One Engine Inoperative (OEI) power to allow an adequately low rate of descent at touchdown for the Rejected Take-Off (RTO) case, and to allow deck edge clearance and subsequent climb away for the Continued Take-Off (CTO).

- iii) Wind Speed. The wind speed over the heli-deck will affect the power required and any head wind component may allow increased weights or require modifications to the piloting strategy.
- iv) View and Helideck Size. The view from the helicopter will be a non-performance related factor that will limit the maximum height for the TDP as the pilot requires to maintain a view of the helideck at all times up to the TDP or the maximum height reached during the reversal of direction necessary during an RTO. It follows that for a given helicopter, the smaller the helideck, the lower the maximum TDP.
- v) Handling Qualities. Severe cross couplings between axes will influence the precision and ease with which the required manoeuvres can be carried out. A significant factor will be the ease with which the relevant power limit (engine or transmission) can be set. This will involve engine response characteristics and indeed the clarity and characteristics of the cockpit instruments the pilot will use.

2.3 The Piloting Strategy for a Towering Take-off

Without giving detailed consideration to all the factors noted in section 2.1, a general strategy that would be valid for many situations operating from a normal size helideck (22.2m diameter) is described below:

- i) Initial Hover. The helicopter would start from a position sitting on the centre of the helideck with the cyclic control and yaw pedals close to central, and the collective lever fully down. To establish the initial hover, collective pitch is applied progressively whilst cyclic and pedal inputs are made to counteract any cross coupling between axes as the helicopter lifts off and to maintain the position over the centre of the helideck. The initial hover height will be 15 ft and the amount of collective applied will depend on the thrust required to achieve that height.
- ii) Vertical Climb. From the initial hover, collective pitch is applied quickly, within approximately 2 seconds, until an engine or transmission limit is reached or the rate of climb is approximately 500 ft per minute. Cyclic and pedal inputs are made as required to maintain position over the centre of the helideck.
- iii) Take-off Decision Point. A likely TDP would be 50 ft as indicated by Radio Altimeter. At the TDP, the pilot would make a positive forward cyclic input to achieve a nose down, accelerative attitude. A usual nose down attitude would be 15 degrees in order to accelerate the helicopter towards the initial climbing speed.

- iv) Acceleration and Climb. After achieving the required nose down attitude at TDP, as speed increases, the pilot allows the nose to rise progressively until the helicopter ceases to accelerate as it reaches the initial climbing speed of 70 knots. The nose will rise due to flap-back caused by the effects of increasing airspeed through the rotor, to pilot longitudinal cyclic inputs, or to a combination of both depending on the characteristics of the particular helicopter. During the acceleration, lateral cyclic and pedal inputs are made to achieve wings level balanced flight. The collective may require adjustment to keep within engine and transmission limits and to establish a desirable initial rate of climb of 1000 feet per minute.

2.4 Piloting Strategy for Recovery from Engine Failure During a Towering Take-off

Having discussed both the piloting aspects and the inverse simulation of the normal towering take-off procedure, the piloting approach in the event of an engine failure is now described before the techniques associated with the inverse simulation of this situation are outlined.

i) Failure Before TDP

The objective on recognising an engine failure before TDP is to reverse the upwards vertical motion promptly, conserve and maintain Nr during a vertical descent and carryout a smooth touchdown on the helideck using all the power available from the remaining engine and stored energy in the rotor. Taking these in turn :

- a) Flight Path Reversal. The pilot will make a rapid downwards collective lever input on recognising the engine failure. The size of the input will depend on the rate of climb at the point of recognition. In general, rate of climb will increase as the vertical climb portion of the towering take-off progresses, so it follows that the larger inputs are required close to the TDP. Cyclic control and yaw pedal inputs are made to compensate for cross couplings to ensure that the helicopter remains over the helideck.
- b) Conserving Nr and Vertical Descent. Once the flight path has been reversed, it will be necessary to conserve adequate Nr and therefore stored energy to cushion the touchdown. To achieve this, the collective is set such that the remaining engine is producing maximum power, usually by reducing Nr by 1% - 2% below the normal governed setting. With this power set, the descent is monitored and cyclic control and yaw pedal inputs are made as necessary to maintain the vertical descent. The rate

of descent will depend on the power deficit and would typically be 800 feet per minute.

- c) Touchdown. The helicopter is allowed to descend vertically as described above until reaching a height of approximately 15 ft above the helideck at which point a large collective-up input is made. The purpose of this is to use rotor kinetic energy to produce additional thrust for a short period of time in order to achieve a smooth touchdown. The point at which the collective input is made depends on the rate of descent and rotor inertia and will vary between helicopter types. After touchdown, the collective is lowered fully.

ii) Failure Just After TDP

The key objectives with an engine failure just after TDP are to ensure rotor speed remains within acceptable limits and to translate from the hover into forward flight. If the performance scheduling is correct, increasing speed reduces the power required to the point where the helicopter will be able to climb using the power available from the remaining engine. Increasing speed also causes a forward translation that is used to ensure that the helicopter misses the edge of the helideck. The pilot action at TDP is to pitch the nose down, typically to an angle of 15 degrees, using a positive forward cyclic input whether or not an engine has failed. If an engine has failed, such that the failure is recognised as or after the forward cyclic input is made, the correct course of action is to continue with the take-off rather than try to land back on the helideck. In this case, the helicopter will follow a descending flight path as speed is gained, and the pilot will have to lower the collective shortly after the engine failure to prevent the rotor speed falling below the acceptable minimum. Some loss of rotor speed is probably desirable as when airspeed is low most rotors are more efficient at lower rotor speed. As airspeed increases, the nose will tend to rise and in any case will be positively raised at, typically, 35 knots to reduce height loss and establish airspeed at that required for the single engine climb, typically 70 knots. The sequence of events can be summarised as :

- a) Engine failure is recognised as forward cyclic is made at TDP,
- b) nose is pitched down to 15 degrees,
- c) collective is lowered to keep Nr within limits,
- d) nose will rise as speed increases and at 35 knots longitudinal cyclic inputs are made to establish speed at 70 knots,
- e) when 70 knots has been established, a steady climb is maintained using maximum engine power.

During this manoeuvre, which involves predominantly longitudinal cyclic and collective pitch inputs, appropriate lateral cyclic and yaw pedal inputs will be made to maintain wings level balanced flight.

iii) Failure Well After TDP

An engine failure well after TDP will have similar objectives to the case above but clearly the closer the helicopter is to the desired climbing speed of 70 knots, the less will be the need for the pilot to increase airspeed by pitching the nose down and the less will be the height loss. The collective lever will, however, have to be lowered to prevent Nr dropping below the acceptable limits.

2.5 The Normal Approach and Landing Manoeuvre

As the in the Towering Takeoff, the validity of the results from any inverse simulation will depend to a large degree on the accuracy of the manoeuvre description. Information from both pilot and regulatory bodies documents [5] has been used to study offshore landing manoeuvres. The piloting perspective on flying the Normal Approach and Landing (with and without engine failures) is now given in the following sections.

2.6 Pilot Aspects of Normal Approach and Landing Manoeuvres

The Normal Approach and Landing is a manoeuvre commonly employed by pilots in helicopter offshore operations as it is a means of landing a helicopter on an elevated helideck while ensuring that at all times the vehicle is capable of surviving a single engine failure. The manoeuvre is defined to allow variations in pilot technique, skill and alertness and is equally applicable to differing vehicle configurations (centre of gravity and mass etc.). Furthermore the flight path and pilot techniques required are suitable for use in adverse weather, night operations, and conditions of single engine failure. Finally the Approach and Landing manoeuvre is valid at the approved WAT (Weight, Altitude, Temperature) condition.

If an engine failure occurs at any point prior to and including the landing decision point (LDP), the pilot may elect to land or to 'go around' by executing a baulked landing. For an engine failure prior to the LDP, this notional point in the manoeuvre must be specified in such a way as to permit acceleration to the baulked landing safety speed, V_{BLSS} at an altitude of no less than 35ft. above the helideck. After passing the LDP, the helicopter no longer has sufficient energy to assure transition to the baulked landing condition without striking the landing surface, and the pilot must continue the landing. Therefore the LDP represents the commit point for the landing manoeuvre in much the same way as the takeoff decision point

(TDP) does in the Towering Takeoff. It is therefore appropriate to specify the LDP in terms of speed, altitude and a descent angle. For Cat. A profiles the LDP is typically 100 -150ft above the landing surface.

A simple, repeatable and effective pilot strategy is borne from the Cat. A requirements and these strategies as understood by the University of Glasgow are now discussed.

2.7 A Possible Piloting Strategy for a Normal Approach and Landing

- a) Initial Descent : The helicopter starts the manoeuvre in a steady trimmed descending flight mode. During the stabilised approach the flight path speed will be typically in the region of 30 - 40 kts, with a descent rate of 300ft/min and this corresponds to a descent angle of approximately 5deg. The vehicle will have a small pitch - nose - up attitude thus ensuring adequate pilot view of the helideck. This steady trimmed flight state is maintained until the landing decision point is reached.
- b) Landing Decision Point: When the vehicle approaches the LDP, a modified flight profile is adopted. At the LDP, the combined use of collective and longitudinal cyclic is used to decelerate the aircraft and increase the descent angle to 10 -15 deg. Typically for this, the aircraft nose is pitched up to a constant value via the long. cyclic and the collective is lowered. The decrease in collective will depend on the initial flight speed and ultimate descent angle. The magnitude of the pitch nose up is determined by the proximity of the rig, initial flight speed and peak descent angle. Lateral cyclic is used to maintain wings level, while pedal displacements are issued to keep the heading constant. Note that a 'crabbing' approach can be employed during this phase to produced enhanced visibility through side view panels.
- c) Flare Point : At the flare point the vehicle is typically 25ft above the landing surface. Flight speed is very low and below that measurable from external pitot fixtures. For this reason visual cues from the rig a very important during this phase. Longitudinal cyclic stick displacements are used to progressively reduce any remaining positive nose up attitude while gradually reducing flight speed. Collective is used to descend the vehicle towards the helideck. Lateral cyclic and pedal displacements are used to maintain wings level and heading as appropriate.

2.8 A Possible Piloting Strategy for a Normal Approach and Landing With an Engine Failure

i) Failure before LDP

On recognising an engine failure, the pilot priorities are to prevent excessive rotor speed decay using remaining engine power, rapidly transition the vehicle to forward flight attaining the baulked landing safety speed and avoid collision with the rig structure by descending to no more than 35ft above the landing surface. Considering these piloting goals the following strategy develops:

- a) The pilot will lower main rotor collective ensuring the rotor speed stays within acceptable limits. Typically rotor speed should not be allowed to drop below 93.5%. Longitudinal cyclic will be used to accelerate the helicopter into a descending forward flight mode. Typically a pitch down nose attitude of 15-20deg will be used to rapidly achieve the baulked landing safety speed of around 41 - 45kts. Lateral cyclic and pedal controls are used to maintain wings level and heading respectively
- b) If the performance scheduling is correct, then as V_{blss} is approached, the remaining good engine should provide sufficient power to prevent excessive loss in altitude. At this point main rotor collective can be increased to reduce descent rate. Furthermore, as flight speed increases, the nose will pitch up due to rotor flap back and positive longitudinal cyclic inputs by the pilot and the helicopter will enter a climbing mode. The baulked landing safety speed is maintain during the subsequent fly away to complete the manoeuvre with a positive rate of climb of approximately 300ft/min.

ii) Failure After LDP

For an engine failure after the LDP, pilot strategy is severely limited by low the energy capabilities of the helicopter and the proximity of the rig structure. Consequently, the resulting strategy is similar to that found during the normal approach and landing except for a more rapid rate of descent being employed during the final touch down phase. The descent has the characteristics of a vertical reject manoeuvre during a towering takeoff as an increased descent rate is adopted (around 800ft/min) and with rotor speed on landing not dropping below 80%.

3. Mathematical Representation of Offshore Flight Paths

The initial mathematical representation of offshore manoeuvres, [7], used single polynomial functions of time to model individual phases of the manoeuvre. That is, for each distinct phase of the manoeuvre, a single matched polynomial function of time was used to specify the variation of altitude, climb rate, velocity or some other suitable manoeuvre parameter. Furthermore the manoeuvre boundary conditions were specified in terms of parameters related to the physical geometry of the trajectory and ignored vehicle performance related aspects of the manoeuvre. These two features of the original mathematical model of the manoeuvres lead to flight path definitions and simulation results that did not fully capture actual piloting strategies. To overcome this, a new approach was adopted that represents the manoeuvre as a series of imposed performance goals.

3.1 A Mathematical Description of the Towering Take-off Manoeuvre

The piloting description given in section 2.1 and 2.2 relate to the Towering Take-off shown in Figure 1 and it is evident that this manoeuvre is defined in terms of four distinct phases. In the following mathematical description the Initial Hover phase is not modelled, partly as this simplifies the overall definition, but also because this is considered as the least critical phase of the manoeuvre. As a consequence of this simplification it is assumed that the manoeuvre is initiated from a hover condition 5m (approximately 15ft) above the helideck. An earth fixed axes set is located at this point with the x-axis pointing in the direction of flight, the z-axis vertically downwards and the y-axis completing a right-handed frame. The inverse simulation requires time histories of the vehicle's velocity and acceleration throughout the manoeuvre related to this axes set [8].

On consideration of both the pilot's comments and the regulatory information [2, 4, 5] it was decided that the most fundamental parameters associated with the towering take-off are the helicopter's velocity and climb rate, and hence the model now described is based on knowledge of these parameters. More specifically it is necessary to specify values for the altitude, h_{TDP} , and vertical velocity, v_{TDP} , at the TDP, and also the flight velocity, V_E , climb angle, γ_E , and altitude, h_E , at some notional exit point. As will become apparent it is also necessary to supply values for the peak accelerations expected during certain phases of the manoeuvre, and the time it is likely to take for the helicopter to reach these values. These figures are performance related and will depend to a large degree on the take-off mass of the vehicle. It is interesting to note that this approach of defining a manoeuvre in terms of performance goals which must be met is adopted by the authors of the U.S. Mil. Spec 8501 Handling Qualities Requirements [9] in their description of Mission Task Elements.

Having specified the vertical velocity and height at the TDP the other two phases (Vertical Climb and Acceleration and Climb) are defined in such a way that they match one another at the TDP to produce a smooth transition.

i) The Vertical Climb Phase ($0 < t \leq t_{TDP}$)

The most convenient approach to modelling the vertical climb phase is to specify a vertical acceleration profile such as that shown in Figure 2(a). In this representation it is assumed that from a trimmed hover condition, the application of collective will cause an increasing vertical acceleration up to some maximum value, \dot{V}_{max} , (depending on the collective setting). As the required vertical velocity, v_{TDP} , is approached the ideal situation is to reduce the vertical acceleration (by lowering collective) to zero hence giving a constant vertical velocity climb. This climbing phase is completed when the TDP height (h_{TDP}) is reached and the vehicle transitions to forward flight. A piecewise smooth polynomial function of time was used to obtain the profile shown in Figure 2(a) for the vertical acceleration. Its construction is given below:

$$\begin{aligned}
 0 < t \leq t_1 & \quad \dot{V}(t) = \left[-2\left(\frac{t}{t_1}\right)^3 + 3\left(\frac{t}{t_1}\right)^2 \right] \dot{V}_{max} \\
 t_1 < t \leq t_2 & \quad \dot{V}(t) = \dot{V}_{max} \\
 t_2 < t \leq t_{CP} & \quad \dot{V}(t) = \left[1 - \frac{3}{2}\left(\frac{t-t_2}{t_{CP}-t_2}\right)^2 + \frac{1}{2}\left(\frac{t-t_2}{t_{CP}-t_2}\right)^3 \right] \dot{V}_{max} \\
 t_{CP} < t \leq t_{TDP} & \quad \dot{V}(t) = 0
 \end{aligned} \tag{1}$$

Cubic polynomial functions were chosen as they have been found to give an adequate degree of continuity whilst being relatively simple to implement. The values of the maximum acceleration, \dot{V}_{max} , and the time for the collective pulse, t_{CP} , must be supplied, and it is assumed that the pulse is symmetrical such that

$$t_1 = t_{CP} - t_2.$$

It is then possible to obtain the value for t_2 by enforcing the condition that at $t = t_{CP}$, the constant vertical velocity v_{TDP} , should have been acquired. This is achieved by integration of the acceleration profile :

$$\int_0^{t_{CP}} \dot{V}(t) dt = v_{TDP}$$

Although on completion of this collective pulse the required vertical velocity will have been reached, it is unlikely that a safe altitude will have been gained. It is therefore assumed that the helicopter continues its vertical climb at constant velocity as indicated in Figure 2(b) until the required altitude, h_{TDP} , is reached (at a time t_{TDP}). This time is readily obtained by noting that in a vertical climb

$$v(t) = \int^t \dot{V}(t) dt$$

and

$$\int_0^{t_{TDP}} v(t) dt = h_{TDP}.$$

A purely vertical climb from the take-off point is ensured by adding the further constraints that

$$\dot{x}(t) = 0 \quad \text{and} \quad \dot{y}(t) = 0,$$

throughout this phase.

ii) The Acceleration and Climb Phase ($t_{TDP} \leq t < t_m$)

After the TDP the helicopter begins to accelerate forward whilst still climbing until the notional exit point is reached. The requirement is to obtain some function which gives a realistic geometrical profile for this phase whilst still satisfying the mathematical constraints imposed by the definition. If we consider first the altitude function, this must satisfy the three conditions already imposed at the end of the vertical climb phase (i.e. at $t = t_{TDP}$, $z = -h_{TDP}$, $\dot{z} = -v_{TDP}$ and $\ddot{z} = 0$), whilst also meeting the requirements at the exit. The exit flight state is a constant velocity, V_E , climb at some angle γ_E , whilst at the exit point the altitude should be h_E . This gives the exit conditions

$$t = t_m, \quad z = -h_E, \quad \dot{z} = -V_E \sin \gamma_E, \quad \ddot{z} = 0.$$

The least degree polynomial satisfying these conditions for the altitude profile, $z(t)$ is therefore a fifth order polynomial, Figure 2(c), where the six constant coefficients are selected to satisfy the six conditions specified above. Note that the choice of a higher order polynomial permits the altitude at the exit point to be directly specified and thereby contributing to the realism of the flight path profile.

The most appropriate way of satisfying the velocity requirement at the exit has proved to be the specification of a longitudinal acceleration profile, $\ddot{x}(t)$. The chosen profile is shown in Figure 2(d), and is identical in form to that used for the acceleration in the vertical climb phase. Consequently, the functions for $\ddot{x}(t)$ are similar to those given by equations (1). This profile gives a rapid change in acceleration from zero up to a maximum value, \ddot{x}_{max} , (as before this value is specified and is related to the performance capabilities of the helicopter) which is maintained until the commanded forward speed is approached and the acceleration is reduced until a constant flight speed is attained. As with the vertical climb, the time taken to achieve maximum acceleration, $(t_3 - t_{TDP})$, and the time taken to establish constant velocity at the exit, $(t_m - t_4)$, must be supplied. It is then possible, given that V_E and γ_E are also known, to obtain a value for the time spent at constant acceleration, $(t_4 - t_3)$, from the expression

$$\int_{t_{TDP}}^{t_m} \ddot{x}(t) dt = V_E \cos \gamma_E$$

The final condition imposed during the flyaway section is that there should be no lateral motion and hence

$$\dot{y}(t) = 0.$$

The definition of the Towering Take-off is completed by the additional constraint that heading should be maintained constant throughout.

It should be noted that previous work on helicopter nap-of-the-earth manoeuvres and Mission Task Elements [10], including comparison between the actual flight trajectories and the polynomial models, has indicated that this approach can give realistic and valid profiles.

3.2 Mathematical Model of the Normal Approach and Landing Manoeuvre

The Normal Approach and Landing manoeuvre is shown in Figure 3. There are three key phases of this manoeuvre evident from the piloting description of the manoeuvre given in section 2.7. The mathematical modelling of these distinct phases of the flight profile can be conveniently overcome by representing the complete manoeuvre as the combination of individual trajectories and this rationale is evident from the formulation of the flight paths given in the next section. A conventional Earth fixed axis set is presupposed. Vertically offset from the initial helicopter position, the z-axis points downward, the x-axis is in the direction of flight and is level with the heli-deck and the y-axis completes the right-handed

triad. The velocity and acceleration time histories used as input for the inverse simulation are related to this axes set.

Examination of pilot comments and the regulatory documents for the Normal Approach and Landing reveals that flight velocity and approach angle are the intrinsic parameters associated with the manoeuvre. The task of modelling the flight path is based on the knowledge of these parameters, however, it is also necessary to specify the velocity, V_{LDP} , the descent rate v_{LDP} , and the height, h_{LDP} , at the landing decision point (LDP). Furthermore the maximum descent angle, γ_{MAX} , and the flare height, h_{FLR} at the flare point must be given. Also it will become apparent that it is necessary to specify the peak deceleration and the time taken to achieve this during the primary deceleration phase.

For these considerations, a mathematical model of a Normal Approach and Landing manoeuvre is now given.

i) Steady Descent Phase ($0 < t < t_{LDP}$)

During the steady descent phase, the vehicle is in a trimmed flight condition and the key piloting parameters are the approach flight speed, V_{LDP} , and rate of descent, v_{LDP} . The flight path velocity and descent rate time histories can be given by,

$$V(t) = V_{LDP}$$

$$v(t) = V_{LDP} \sin \gamma_{LDP}$$

where γ_{LDP} is the LDP descent angle. The landing decision point height is assured by integration of the descent rate profile:

$$h_1 - \int_0^{t_{LDP}} v(t) dt = h_{LDP}$$

where h_1 denotes the initial manoeuvre height.

ii) Primary Deceleration Phase ($t_{LDP} < t \leq t_{FLR}$)

During the period of the manoeuvre from the landing decision point to the final flare altitude, it is assumed that a constant deceleration phase is adopted. The most appropriate way of achieving this is by specifying a longitudinal acceleration time history, $\ddot{x}(t)$. A transient deceleration phase must also be specified to transition the helicopter from its

trimmed flight mode at the LDP to some maximum constant deceleration, \ddot{x}_{\min} , at time t_1 . The time t_1 is selected to suit the nature of the manoeuvre, while a smoothly connected, piecewise cubic polynomial in time was chosen to achieve the transition. Figure 4a. The longitudinal acceleration can then be expressed as,

$$\begin{aligned} t_{\text{LDP}} < t \leq t_1 & \quad \ddot{x}(t) = \ddot{x}_{\min} \left[-2 \left(\frac{t - t_{\text{LDP}}}{t_1 - t_{\text{LDP}}} \right)^3 + 3 \left(\frac{t - t_{\text{LDP}}}{t_1 - t_{\text{LDP}}} \right)^2 \right] \\ t_1 < t \leq t_{\text{FLR}} & \quad \ddot{x}(t) = \ddot{x}_{\min} \end{aligned}$$

As in the Towering Takeoff manoeuvre, cubic polynomials were chosen as they provided adequate continuity whilst being simple to implement.

In addition to specifying the acceleration time history, the nature of the piloting strategy indicates that descent angle should also be defined. It is assumed in this model of the Approach and Landing manoeuvre that descent angle increases from γ_{LDP} to some maximum value γ_{MAX} over the period t_{LDP} to t_1 . The descent angle, γ_{MAX} , is maintained until the flare point is reached. As in the expressions for $\ddot{x}(t)$, a cubic polynomial function of time was used to achieve the transition in descent angle. The functions required for variation in descent angle can be given as,

$$\begin{aligned} t_{\text{LDP}} < t \leq t_1 & \quad \gamma(t) = (\gamma_{\text{MAX}} - \gamma_{\text{LDP}}) \left[-2 \left(\frac{t - t_{\text{LDP}}}{t_1 - t_{\text{LDP}}} \right)^3 + 3 \left(\frac{t - t_{\text{LDP}}}{t_1 - t_{\text{LDP}}} \right)^2 \right] + \gamma_{\text{LDP}} \\ t_1 < t \leq t_{\text{FLR}} & \quad \gamma(t) = \gamma_{\text{MAX}} \end{aligned}$$

and shown in Figure 4b.

In this formulation of the Normal Approach and Landing manoeuvre, the maximum descent angle is specified. Recalling that the longitudinal velocity profile, $\dot{x}(t)$, can be obtained from,

$$\dot{x}(t) = \int^t \ddot{x}(t) dt$$

then the peak deceleration value, \ddot{x}_{\min} , can be chosen to ensure that the flare height is achieved from,

$$h_1 - \int_0^{t_{\text{FLR}}} \dot{x}(t) \tan \gamma(t) dt = h_{\text{FLR}}$$

iii) Final Flare Phase ($t_{FLR} < t \leq t_m$)

As the helicopter enters the final flare phase, the requirement is for the vehicle simultaneously decelerate until the ground velocity becomes zero while reducing altitude until the helicopter lands on the helideck. At the flare point, a cubic polynomial of time is used to vary the deceleration from its maximum value, \ddot{x}_{min} , to zero over the period t_{FLR} to t_m . The function required for this is given as,

$$t_{FLR} < t \leq t_m \quad \ddot{x}(t) = -\ddot{x}_{min} \left[-2 \left(\frac{t - t_{FLR}}{t_m - t_{FLR}} \right)^3 + 3 \left(\frac{t - t_{FLR}}{t_m - t_{FLR}} \right)^2 \right] + \ddot{x}_{min}$$

and is shown in Figure 4c. The duration of the final flare phase is chosen to reflect the proximity of the oilrig platform and is a feature of the mathematical model.

Considering the altitude function, the boundary conditions at the flarepoint and at the end of the manoeuvre are given as,

$$\begin{array}{llll} \text{a) } t=t_{FLR} & z = -h_{FLR} & \dot{z} = \dot{z}_{FLR} & \ddot{z} = \ddot{z}_{FLR} \\ \text{b) } t=t_m & z = 0 & \dot{z} = -v_E & \ddot{z} = 0 \end{array}$$

The final rate of descent at the exit of the manoeuvre is denoted by, v_E . A fifth order polynomial function in time, $z(t)$, was selected for the altitude profile, Figure 4d, where the six coefficients are chosen to satisfy the six boundary condition specified above.

The Normal Approach and Landing is a pure longitudinal manoeuvre and thus the final constraint is simply given by,

$$\dot{y}(t) = 0$$

The definition of the Normal Approach and Landing is completed by specifying the additional constraint that the heading should be maintained constant throughout.

4. Modelling Developments

Over the past twelve months research, two important areas of the helicopter mathematical model have been enhanced. Firstly, a model of a twin engine powerplant of the free - turbine type has been included. Secondly, an automatic stability and flight control system has been provided. These enhancements are now discussed.

4.1 Twin Engine Model

The inverse simulation algorithm uses the helicopter mathematical model HGS (**H**elicopter **G**eneric **S**imulation) [6]. The engine model initially incorporated in HGS is based on that described in Reference 11. For the current study involving engine failures, it has been necessary to replace the original single engine model with a twin engine version where either engine can be failed separately. This has been achieved by duplicating the original model, retaining its structure but adjusting the values of its parameters so that the combined model functions exactly as the original [12]. That is, the time constants of its dynamics are identical but the torque produced by each engine is half of the original with the fuel intake being equally shared. Engine failure is simulated by setting the fuel flow of the failed engine to zero, so that its contribution to the overall torque falls to zero in a realistic manner. The unaffected engine increases its contribution to the torque to compensate for the failure as shown in Figure 5. At the same time, the opportunity has been taken to introduce some realistic non-linearities into the engine model by incorporating a torque limitation based on setting a maximum allowable fuel flow.

The mathematical model of the twin engine, torque limited powerplant is shown in Appendix 1.

4.2 Artificial Stability and Flight Control System

Most helicopters have some form of artificial stability included, whether it is in the form of a mechanical gyro device which is an integral part of the rotor head or a electromechanical system that is based on signals from attitude or rate gyros. The artificial stability system adopted in this study is of the electromechanical type presented by Padfield [11]. The autostabiliser contributions to the cyclic and tailrotor channels are obtained from proportional and derivative action feedback signals derived from rate and attitude gyro's. The cyclic autostab channel also has an additional feed forward term to improve vehicle response. The autostabiliser contribution to collective is obtained from the feedback of the signal from a normal accelerometer. The flight control system transmits the pilot collective, cyclic and pedal inputs to the main and tail rotor swashplate. A series of primary control

links is used to achieve this. In addition, control interlinks between collective, longitudinal cyclic and pedal displacements are incorporated to reduce pilot workload. The autostab and pilot control signals are combined before being passed through hydraulic actuators. Prior to actuating the main rotor blades, the cyclic pitch displacements are mixed to reduce pitch - roll cross coupling effects.

The mathematical model of the autostab and flight control system is described in detail in Appendix 4.

5. Simulation Developments

In order to perform simulated studies of offshore operation that include an engine failure, three crucial simulation advancements have been made and these are now presented.

5.1 Inverse - Forward - Inverse Simulation

In addition to developing an engine model which can replicate failures, it is also important to incorporate the event of an engine failure into the context of the manoeuvre simulation in a realistic manner. Earlier sections of this report have described the general approach of specifying flight paths as trajectories defined via piecewise polynomials connected with an appropriate degree of continuity, and calculating, from the helicopter mathematical model, the pilot's control movements - or in general terms - strategy. The modelling view of this situation is that of the pilot anticipating the control movements needed to accomplish the manoeuvre as the flight path is traversed. However it is clear that when an engine fails he cannot instantaneously adjust his strategy to the modified performance of his vehicle. That is, until he has recognised and reacted to the failure, his strategy will be that consistent with the original manoeuvre. After the elapse of the reaction time, he will adopt a new strategy - either planning to return to the original flight path or mentally redefining his piloting goals and preparing a strategy leading to a new trajectory. This adaptation of the pilot to the new circumstances is captured in the current work by successive intervals of inverse simulation, forward simulation and inverse simulation. The first period of inverse simulation takes the pilot up to the failure point in the normal manner of inverse simulation described earlier. In the second period, the helicopter is flown with its engine failed but a control strategy based on its original manoeuvre; it is this second interval which emulates the reaction time of the pilot. In it, the pilot is acting according to the original strategy for the helicopter whereas the helicopter is responding with its modified performance. Naturally this will lead to a divergence of the helicopter from its flight path as originally defined and in the next phase of the manoeuvre the pilot reacts to the new situation by adopting a strategy which ultimately leads to a new recovery flight path or a return to the original.

In order to mirror authentically the different phases of a manoeuvre incorporating engine failure, a new simulation package has been developed. It is one which can perform inverse simulation up to a certain point in time and then switch to normal forward simulation, using the control inputs that would have been calculated for a continuation of the inverse simulation. After a specified interval of time (the reaction time) the simulation reverts to inverse simulation in order to adopt a new flight path for the continuation of the flight - either to return to the original manoeuvre or to pursue a different strategy - for example by descending in order to build up a safe flying speed.

5.2 Development of Blending Functions

It is necessary to ensure a realistically smooth transition between the different phases of the simulation. The first transition, from inverse to forward is naturally smooth since the initial values of the state variables for the forward simulation are available from the final point of the inverse simulation. The second, from forward to inverse, requires a smooth transition from its diverged flight path to the new one. In addition, the supplementary constraint, in this case a prescribed heading, may be violated during the forward phase so that its return to that required in the inverse phase must be introduced smoothly. Part of the current work has been to study the effect of bringing the departures of the variables back to zero with varying degrees of severity and the development of techniques for ensuring a smooth transition have included a parameter to control the rate at which the new flight path is captured.

The requirement is for a function $h(t)$ to blend smoothly from $f(t)$, the current flight path, to $g(t)$, the target flight path over an interval $t = t_{pr}$ (the time at which the pilot responds to the engine failure) to $t = t_R$ (the time at which the recovery trajectory is achieved) as illustrated in Figure 6. Let $h(t) = g(t) + \phi(t)$, and let the required degrees of derivative continuity at $t = t_{pr}$ and $t = t_R$ be M and N respectively, then:

$$h^m(t_{pr}) = g^m(t_{pr}) + \phi^m(t_{pr}); \quad \text{for } m = 0 \text{ to } M$$

and

$$h^n(t_R) = g^n(t_R) + \phi^n(t_R); \quad \text{for } n = 0 \text{ to } N$$

so that ϕ satisfies:

$$\phi^m(t_{pr}) = h^m(t_{pr}) - g^m(t_{pr}) \quad \text{for } m = 0 \text{ to } M$$

and

$$\phi^n(t_R) = 0; \quad \text{for } n = 0 \text{ to } N.$$

Now bias the blend by writing $\phi(t) = e^{-\delta t} p(t)$, for some polynomial $p(t)$, from which it is easy to write:

$$\phi(t) = e^{-\delta t} p(t)$$

$$\phi'(t) e^{-\delta t} + \delta \phi(t) e^{-\delta t} = p'(t)$$

$$\phi''(t) e^{-\delta t} + 2\delta \phi'(t) e^{-\delta t} + \delta^2 \phi(t) e^{-\delta t} = p''(t)$$

....

$$e^{\delta t} \sum_{M=C_r} \phi^{(r)}(t) \delta^{(M-r)} = p^{(M)}(t)$$

where r is the highest degree of derivative continuity required at the merging points. The biasing of the blend gives the required parameter to adjust the speed at which the new trajectory is adopted - where 'new' includes the case where the original trajectory is rejoined. To illustrate this Figure 7 shows the effect on the trajectory of an engine failure where no action has been taken by the pilot for 5 seconds. This is of course an unrealistic reaction time but does clearly demonstrate departure from the originally defined trajectory. The final trajectory is one of similar slope to the original but at a lower altitude, and the effect on the blending function of varying the bias, δ , is clear from this plot - higher values allowing the final condition to be acquired earlier. The type of blending described above is used for the trajectory co-ordinates x , y and z and in addition the applied constraint- either heading or sideslip, and there is the opportunity if so desired to use different values of δ for different variables where, for example, it may be desirable to bring the heading round to a preferred direction as a priority above that of the velocity components. In the current work the degree of continuity imposed at each end is three so that $p(t)$ is a polynomial of degree five.

6. Helicopter Offshore Graphical Simulation (Hogs)

To aid the current research, a computer generated, three dimensional, helicopter offshore environment has been created on a Silicon Graphics Iris Indigo XS workstation. Oil rig platforms, tug boats, and mountain scenery have been provided to enhance realism and visual cueing. A helicopter typical of those found in offshore operations has also been created. A computer generated scene from the Hogs environment is shown in Figure 8. The user interface is via a 'mouse control', allowing the helicopter motion to be viewed from any position. The Hogs software package requires flight path co-ordinates and Euler attitude angles as input from Helinv.

The geometries in the simulated environment are modelled using elemental, single coloured, flat surfaced, simple polygons. Geometric shapes such as the cylinders that represent the oilrig legs use a triangular meshing technique that can be readily incorporated into efficient drawing algorithms. Because of the complex nature of the helicopter surface, it was exclusively formed from user defined flat surfaced polygons of four vertices. The three dimensional surface co-ordinates necessary for the specification of the polygon vertices were obtained from scaled drawings of a suitable helicopter. The main and tail rotors of the helicopter were represented as a series of elemental polygons of varying colour, transparency and intensity. This method places reduced loads on the limited processor power available and provides a realistic image of the rotating rotor. Real-time operation is ensured due to a 'hardware - software' link that monitors both the run and flight time.

7. Qualitative Validation and Analysis of Results

7.1 Inverse Simulation of the Towering Take-off Manoeuvre

It is necessary to provide only a few basic parameter values to use the definition of the Towering Take-off given above. In the following example the parameter values are

$$\begin{aligned}
 h_{\text{TDP}} &= 10\text{m}, & v_{\text{TDP}} &= 2.5 \text{ m/s} (\equiv 500\text{ft/min}), & \dot{V}_{\text{max}} &= 2 \text{ m/s}^2, & t_{\text{CP}} &= 2 \text{ s} \\
 \ddot{x}_{\text{max}} &= 3 \text{ m/s}^2, & t_3 - t_{\text{TDP}} &= 2.5\text{s}, & t_3 - t_m &= 14\text{s}, & V_E &= 70 \text{ knots}, & h_E &= 70\text{m}, \\
 & & & & & & \gamma_E &= 8 \text{ deg} (\equiv 1000\text{ft/min at 70 kts}).
 \end{aligned}$$

These values are representative of those routinely encountered during take-off from offshore installations. Note that the TDP height is referred from the starting height of the climb (5m) and therefore represents an altitude of 15m above the helideck. Time histories of several of the flight path variables are shown in Figure 9. The time to reach TDP is 5 seconds and the manoeuvre completion time is approximately 25 seconds. From the vertical acceleration profile, the initial pulse takes 2 seconds (as indicated by the piloting description given in section 2.2(ii)) by which time the vertical velocity is 2.5 m/s. The TDP is reached at about 5 seconds, after which the acceleration and climb phase begins with a rapid increase in forward acceleration, the maximum value being set at 3 m/s² to be reached after 2.5 seconds. The velocity increase in conjunction with the relatively slow initial increase in height leads to a rapid decrease in climb angle from 90 degrees at the TDP to a value slightly below the required exit condition of 8 degrees at approximately 15 seconds. Thereafter, as the required constant velocity is approached, and the climb rate begins to increase, and the climb angle slowly increases towards its final constant value. The resulting flight path trajectory is also shown in Figure 9.

This manoeuvre information may be used to drive the Helinv inverse simulation thereby producing time histories of the helicopter's states and controls. The helicopter configurational data used in this paper is characteristic of a large transport vehicle of the class likely to be employed in offshore operations. A brief summary of this data is given in Table 1.

| Parameter | Value |
|---------------------------------------|--------|
| Aircraft Mass (kg) | 9000 |
| Rotor Radius (m) | 9.5 |
| Rotor Solidity | 0.0363 |
| Flapping Stiffness (kNm/rad) | 160 |
| Maximum Power Output (SHP) | 2800 |
| Rotor Speed at Flight Idle (rad/s) | 22 |

Table 1 : Leading Parameters for Transport Helicopter Configuration

The inverse simulation results for the transport configuration flying the towering take-off described above are shown in Figure 10. The vertical climb section of the manoeuvre is clearly visible from these plots : over the first 5 seconds there is little cyclic motion and hence little change in attitude, whilst at the same time there is firstly a pulse in collective lever to produce the desired vertical acceleration, followed by an offset in collective setting from the trim position producing the constant vertical velocity climb. The effect of the collective pulse on engine torque and rotor speed are also apparent with both engines peaking at about 95% of their maximum torque, and the rotor speed falling by a small amount. After the TDP there is a pulse in forward cyclic stick of 25% to induce a nose down pitch attitude of about 15 degrees in order to achieve the commanded forward acceleration. After this pulse there is a short aft stick pulse to arrest the nose down motion followed by a more sustained but slow forward stick motion to account for the disc flapping backwards as forward speed is increased. The nose down attitude is maintained until about 12 seconds at which point a slow aft stick motion begins to raise the nose. Note that the stick forward pulse which initiates the acceleration is much more aggressive than the subsequent stick back motion - this is to reflect the likely piloting strategy of clearing the helideck as quickly as possible after the decision to climb away has been taken. During the acceleration and climb phase the collective is initially increased to produce the desired climb rate, but is subsequently reduced towards the end of the manoeuvre as speed increases, and the desired flight state is reached. With the reduction in collective, the engine torque and power fall whilst the rotor speed increases slightly. It is also noticeable from Figure 10 that there are only very small changes in the lateral cyclic position and roll attitude, whilst there is a gradual change in pedal position as forward speed is increased.

Comparing the discussion above with the piloting comments in section 2.2 and 2.3 it is clear that the key features of an initial 2 second pulse in collective and a subsequent pulse in forward cyclic leading to a 15 degree pitch down attitude are correctly predicted by the

inverse simulation through its defined trajectory. The manoeuvre as defined reaches about 95% of nominal maximum torque and therefore complies with the AEO requirement in section 2.3(i). The conclusion is that the methods employed have satisfactorily captured the piloting strategy of the normal Towering Take-off procedure. The more complex situation of the failure of an engine during take-off is now considered.

7.2 Inverse Simulation of Engine Failures During Towering Takeoff

The simulation results presented in this section are for the transport helicopter described in Table 1. After its failure it is assumed that the engine is shutdown immediately by some automatic system, and that the pilot responds to this failure after a further 1 second. For all 3 cases the initiated manoeuvre is identical to that described in sections 7.1 and shown in Figure 9, and hence, up to the point where the engine has failed and the pilot has responded, the control inputs are as given in Figure 10. An appropriate function is then blended from the point of pilot reaction, to a defined exit condition as described in section 5.3, and the control inputs required to fly this path are calculated. It should be noted that the representation of the engine governor in the simulation is configured such that rotor overspeed is prevented by reducing engine torque when rotorspeed reaches its flight idle limit. This feature can be observed in some of the plots discussed below. In the simulations the torque supplied by an engine is limited to a contingency maximum 15% above its nominal limit. This value corresponds to the OEI value referred to in section 2.2(ii).

a) Failure Before TDP

For this case the engine failure occurs 1 second before the TDP (i.e. 4 seconds into the manoeuvre) and recovery is by means of a rejected take-off, landing back on the heli-deck. This give the following exit conditions

$$h_E = -5\text{m}, \quad v_E = -1.5 \text{ m/s } (\equiv -300 \text{ ft/min}).$$

Note that the manoeuvre is initiated from a height of 5m above the helideck (15ft. approx.) and hence the final altitude of -5m places the helicopter back on the platform deck. The results from this simulation are given in Figure 11. The pilot's reaction (at 5 seconds) to the engine failure in this case is to reduce collective to conserve rotorspeed and arrest the upward motion. The upwards travel of the helicopter is completed at about 6.5 seconds just after collective reaches its minimum position and rotorspeed levels off. There is then a gradual increase in collective as the helicopter descends (causing rotorspeed to fall slowly) followed at about 10 seconds, as the deck is approached, by a much faster increase in collective (and decrease in rotorspeed) to cushion the touchdown. After the failure of the

engine the torque of the remaining engine rises to its contingency maximum and remains there until the manoeuvre terminates.

There is good agreement with the piloting description of section 2.4(i). The decrease of collective results in Nr being maintained within 3% of its reference value until it is dissipated in the final increase of collective applied in order to minimise the impact on touch down. The maximum rate of descent is approximately 800ft/sec, as required.

b) Failure Just After TDP

For this case the simulated engine failure occurs 1 second after the TDP (i.e. 6 seconds into the manoeuvre) and the recovery from this initially follows the nose down acceleration of the normal take-off, but is then followed by a much slower climb from below the level of the platform. The demanded exit condition in this case is

$$h_E = -25\text{m}, \quad V_E = 70 \text{ knots}, \quad v_E = 1.5 \text{ m/s } (\equiv 300 \text{ ft/min}).$$

Note that the given exit height is a displacement from the starting point of the manoeuvre (5m above the deck) and therefore represents a location approximately 20m below the level of the heli-deck. The simulation results are shown in Figure 12. The pilot's response occurs during the normal initial pulse of longitudinal cyclic which initiates the acceleration. The first action taken is to apply a second sharp pulse in cyclic to reinforce the nose down pitch attitude (in this case to 20 degrees) to ensure the deck edge is cleared. This input is accompanied by a rapid drop in collective to maintain rotor speed. The lower collective settings in this case takes the helicopter to a much lower altitude, and combined with smaller longitudinal cyclic inputs produces a much lower rate of climb than in the normal take-off. The effect of the engine governor is clearly visible with the engine torque being reduced when the rotor speed exceed its flight idle value. Two intervals may be observed when the torque of the good engine reaches its contingency limit. The first begins just after failure, and as a consequence the rotor decelerates as the kinetic energy is absorbed to compensate for the torque deficit needed to initiate the next stage of the manoeuvre. After a further 1.5 seconds, the strategy of reducing the collective begins to pay dividends and surplus torque is available to accelerate the rotor back to its reference speed - which it reaches 1.5 seconds later. The demands of the climb-out phase produce the second interval of torque limiting later in the manoeuvre (between 17 and 24 seconds of the elapsed time) and again the plot of the rotor speed shows the initial surrender of kinetic energy to exigencies of the trajectory and its restoration as the manoeuvre severity ameliorates.

Again the results of the simulation may be seen to be generally consistent with the description of section 2.4(ii). As a result of the decrease of collective pitch the rotor speed is generally maintained at its reference value apart from the transitory reductions to 3% below nominal during the periods of torque limiting noted above. The pulse of cyclic to give forward pitch is a little larger in this case to give an accelerated entry into the descent phase.

It is worth noting that the flight path reveals this to be close to the limiting case for this type of manoeuvre. There are two intervals of torque limitation during which the rotor speed falls significantly and the recovery flight path, in reality, would be close to the surface of the sea.

c) Failure Well After TDP

For this case the simulated engine failure occurs 10 seconds after the TDP (i.e. 15 seconds into the manoeuvre) and recovery from this position is achieved by continuing with the take-off but assuming a lower climb rate and velocity. The demanded exit condition is

$$h_E = 50 \text{ m}, \quad V_E = 50 \text{ knots}, \quad v_E = 1.5 \text{ m/s} (\equiv 300 \text{ ft/min}).$$

Referring to Figure 13, there is little cyclic activity required to assume the adopted recovery manoeuvre. The main action is a reduction in collective associated with the adoption of a less demanding climb-out trajectory, so as to prevent an unacceptable droop in rotor speed. The feature of the torque reaching its contingency limit may be observed again in the interval 16 to 24 seconds of the manoeuvre. In this case the rotor speed falls by more than 6% before excess torque is available to begin to recover the nominal rotor speed. Note that the step changes in engine torque produce corresponding step changes in pedal to balance the rotor torque, and a lessening in the rate of reduction of collective. The plot of the flight paths shows quite clearly how the reduction in available engine torque leads to a much lower flight velocity and rate of climb. The simulation results are consistent with the piloting description of section 2.4(iii).

7.3 Inverse Simulation of Normal Approach and Landing

The mathematical representation of the Approach and Landing manoeuvre requires only a few basic parameters with which the flight path, velocity and acceleration time histories can be evaluated. These are :

$$V_{LDP} = 35 \text{ kts}, \quad h_{LDP} = 30.5 \text{ m} (100 \text{ ft.}), \quad v_{LDP} = 2.5 \text{ m/s} (300 \text{ ft/min}) \\ \ddot{x}_{MIN} = 1.25 \text{ m/s}^2, \quad t_1 - t_{FLR} = 2.5 \text{ s}, \quad \gamma_{MAX} = 10^\circ$$

$$h_{FLR} = 25\text{ft.}, V_{FLR} = 9\text{kts}, t_m - t_{FLR} = 9\text{s.}$$

$$t_m = 24\text{s}, v_{TM} = 2.5\text{m/s (300ft/min).}$$

These values are representative of those values found during Normal Approach and Landing manoeuvres to offshore platforms.

The first 4 seconds of the manoeuvre correspond to the initial approach, a phase where constant flight speed and rate of descent are adopted and this strategy is evident from Figure 14. When the landing decision point (LDP) is reached, the primary deceleration phase is entered and spans the period $t = 4 - 15\text{s}$. At the LDP, the descent angle is gradually increased to a value 10° over a period of 2.5s and combined with the high initial approach speed, leads to an initial increase in descent rate to a peak value of 3m/s. From the acceleration time history a rapid increase in deceleration to 1.25m/s^2 is achieved 2.5 seconds after the LDP. Furthermore this value of deceleration is sustained for 9s until the flare point is reached 15.5 seconds into the manoeuvre. The constant deceleration results in velocity decreasing linearly over the primary deceleration phase and this is clear from the velocity time history. At the flare point 25ft. above the helideck and 30ft. from the landing point, a flight speed of 9kts. is attained. For the remaining 8 seconds left until the end of the manoeuvre, flight speed is gradually reduced until the final flight velocity of 2kts obtained on touchdown. The rapid increase in descent rate with gradual reduction in flight velocity results in a rapid increase in descent angle to 90° at the end of the manoeuvre as seen in the descent angle time history.

Once the trajectory information has been calculated, it can then be used as input to the inverse simulation to obtain the corresponding vehicle control displacements necessary for the helicopter to follow the flight path. A helicopter configuration relating to a medium weight transport aircraft as commonly found in offshore operations has been adopted for this study. The controls and flight states generated for such an aircraft flying a Normal Approach and Landing manoeuvre are now discussed.

The inverse simulation results of a Normal Approach and Landing manoeuvre. Figure 15, as represented by the flight path information given in the previous section are now discussed. The steady descent section is clearly visible from the plots and has a duration of 4 seconds. The cyclic stick is close to centre and the body attitudes reflects this - fuselage roll angle is small while the vehicle is pitched 2.5° up affording good pilot vision of the landing platform. The main rotor collective is at a low setting due to the limited demands of the flight profile and consequently the engine torque output is less than 40%. The pedal displacement is sufficient to maintain heading. At the landing decision point, the accelerative demands of the flight path results in the main rotor collective being lowered and longitudinal

cyclic moved aft by 20%. An additional forward pulse of longitudinal cyclic arrests the rotor discs aft motion and results in the vehicle achieving a steady 10° nose up attitude. As the vehicle decelerates, main rotor collective progressively increases to reduce the descent rate. Furthermore, as the forward motion of the helicopter reduces, there is a tendency of the rotor disc to pitch forward and therefore a slow progressive aft motion of the longitudinal cyclic is necessary to maintain the deceleration. During this period the vehicle nose follows the longitudinal cyclic motion and gently pitches upward to a maximum value of approximately 12° at after 15 seconds. At the flare point the collective is set to 40% and a small input in forward cyclic initiates a nose down pitching motion that gently and smoothly reduces the helicopter pitch attitude over the remaining 9 seconds of the manoeuvre. This attitude change is in sharp contrast to that experienced during the initial deceleration and is a feature of the model that reflects the pilot awareness of the rig structure. As ground speed falls to below 1kt. the helicopter enters the final vertical descent phase 14ft. above the ground. Vertical velocity is increased slowly until a final rate of descent of 300ft/min is achieved to complete the manoeuvre. It is also evident from Figure 15 that there is little roll and lateral cyclic motion throughout the manoeuvre and that pedal displacement gradually reduce over the flight.

7.4 Inverse Simulation of Engine Failures During Normal Approach and Landing Manoeuvres

i) Failure Before LDP

For this case, the engine failure occurs at the LDP, that is 4 seconds into the manoeuvre. Pilot response time is taken to be 1 second and the recovery is by means of a baulked landing manoeuvre that transitions the helicopter from the approach trajectory to some climb - out flight path in a smooth and safe manner. The baulked landing safety speed is specified to be 45kts. and the manoeuvre is completed when the aircraft achieves a positive, steady rate of climb of 300ft/min. The simulation results are shown in Figure 16.

The response to the engine failure at 5 seconds by a series of rapid longitudinal cyclic stick inputs that characterise the helicopters acceleration from approach to baulked landing safety speeds. The recovery trajectory is entered via a forward pulse of longitudinal cyclic of approximately 45% which results in a 10° pitch down attitude after 1.6 seconds. The rapid aft motion of the cyclic after the initial pulse prevents excessive forward tilt of the rotor disc, while the subsequent secondary forward longitudinal cyclic stick pulse at 6.5 seconds assures constant flight path acceleration. After the peak nose down attitude has been achieved, longitudinal stick is relaxed and the aircraft immediately pitches upward over a period of 3.5 seconds to a final pitch up attitude of 2.5°. In conjunction with the cyclic stick displacements

used in response to the engine failure, the pilot increases main rotor collective sharply by almost 20% to prevent excessive height loss and meet the acceleration requirements of the trajectory. Once the vehicle has reached its maximum pitch down attitude, collective is increased further by 8% and thus ensuring the descent motion of helicopter is arrested 5 seconds after the engine failure is recognised. The maximum height loss is 8m, while the helicopter overflies the rig at an altitude of 22m and flight velocity of 45kts with a climb rate of 80ft/min. After the single engine failure, the remaining good engine reaches a transient peak torque output of 110%. As the baulked landing safety speed is achieved, the torque output decreases to 90% for the remainder of the manoeuvre. During the complete manoeuvre rotor speed is tightly constrained to its reference value.

The results of the simulation generally compare well with the description of the manoeuvre given in section 2.6(i). A consistent pitch down attitude is obtained during the transition from the approach to baulked trajectories. Furthermore the baulked landing safety speed is achieved as the minimum altitude in the trajectory is reached. The single remaining engine provides sufficient torque to keep rotor speed within specified operating limits. Finally, the approach manoeuvre and subsequent recovery strategy, quite clearly comply with the BCAR [5] requirements of a baulked landing in the event of a single engine failure up to and including the landing decision point.

ii) Failure After LDP

In this example of an engine failure after the LDP, the failure is assumed to occur 4 seconds into the manoeuvre with the pilot response time specified again as one second. The recovery trajectory takes the form of a smooth transition back to the original flight path until the landing manoeuvre is completed. The inverse simulation results are shown in Figure 17.

The response of the pilot with respect to engine failure is small with only some relaxation of the right pedal being used to counteract any adverse nose - left - yaw tendency of the aircraft. The pitch and roll attitude response of the helicopter is very similar that found in case where no engine failure occurs. The engine failure can be clearly be seen from the engine torque time histories. The remaining good engine responds by increasing its torque output by 20% while the rotor speed remains tightly governed. Clearly the torque excess of the remaining engine is sufficient to meet the exigencies of the manoeuvre. As the manoeuvre progresses beyond the pilot response time, cyclic, collective and pedal displacements exhibit the same piloting strategies as those found in the case where no engine failure occurs. From the torque plot, however, the decreasing descent rate and flight speed puts increasing demands on the powerplant and thus the remaining engine torque output steadily increases beyond its normal operating limit to a maximum value of 110%.

approximately 9.5 seconds after the engine failure. At the same time as engine torque output reaches its limiting value, main rotor speed starts to decay and this is clear from the plot. Consequently main rotor collective increases beyond levels found in an Approach and Landing where no engine failure occurs. As the manoeuvre continues, rotor speed decays further with main rotor collective reaching a maximum value on touch down of 85%.

The simulation results compare well those discussed in section 2.8(ii). The collective lever stays within its specified limits while the final rotor speed is very similar to that found during a vertical reject manoeuvre.

8. Conclusions

The success of capturing the important features of piloting strategy and helicopter performance in Towering Take-off and Normal Approach and Landing manoeuvres (with and without engine failures) has provided an encouraging foundation for future studies involving the investigation of pilot strategies in winds and gusts.

For the work reported in this report several specific conclusions may be drawn:

- i) Piecewise description of the different phases of the Towering Takeoff and Approach and Landing manoeuvres has resulted in a trajectory description which acceptably predicts a typical piloting strategy. A blending parameter allows the effect of different recovery strategies to be investigated.
- ii) The development of a combined inverse/forward/inverse simulation package has allowed pilot reaction time to be included in the study in a natural manner.
- iii) The simple twin engine model adequately predicts the surrender of rotor kinetic energy when torque limits are reached - so that the avoidance of excessive rotor speed droop may be used as a criterion for manoeuvre design and piloting strategy.
- iv) The use of dynamic graphics can provide a useful tool in visualising complex flight paths in terms of piloting strategies.

Acknowledgements

The research described in this paper is funded by the U.K. Civil Aviation Authority through an ARB Fellowship Award.

References

1. Taylor, C., Thomson, D.G., Bradley, R., "Rotor Inflow Modelling Enhancements to Helicopter Generic Simulation Mathematical Model", University of Glasgow, Department of Aerospace Engineering, Internal Report 9215, September 1992.
2. Talbot, N., Private Communication, July 1993.
3. Wright, D., Private Communication, October 1993.
4. Anon, "Certification of Transport Category Aircraft", U.S. Department of Transport, Advisory Circular, Federal Aviation Administration, Sept. 1987.
5. Anon, "British Civil Airworthiness Requirements Part 29", Civil Aviation Authority
6. Thomson, D.G., "Development of a Generic Helicopter Mathematical Model for Application to Inverse Simulation", University of Glasgow, Department of Aerospace Engineering, Internal Report 9216, June 1992.
7. Taylor, C., Thomson, D., Bradley, R., 'The Mathematical Modelling of Helicopter Offshore Manoeuvres', University of Glasgow, Department of Aerospace Engineering, Internal Report 9216, June 1992.
8. Thomson, D.G., Bradley, R., "Development and Verification of an Algorithm for Helicopter Inverse Simulation", Vertica, Vol. 14, No. 2, May 1990.
9. Anon, "Aeronautical Design Standard, Handling Qualities Requirements for Military Rotorcraft", ADS-33C, Aug. 1989.
10. Thomson, D.G., Bradley, R., "The Modelling and Classification of Helicopter Combat Manoeuvres", Paper 5.9.1, Proceedings of the 17th ICAS Conference, Sept. 1990.
11. Padfield, G.D., "A Theoretical Model for Helicopter Flight Mechanics for Application to Piloted Simulation", Royal Aircraft Establishment, TR 81048, April 1981.
12. Taylor, C., Thomson, D.G., Bradley, R., "The Simulation of Recovery Procedures from Engine Failures During Helicopter Offshore Operations", University of Glasgow, Department of Aerospace Engineering, Internal Report 9310, July 1993.

Appendix 1

A1. Mathematical Formulation of Twin Engine Power Plant

The twin engine, torque limited, model, is a development of Padfield's single engine model [11]. In the single engine power plant, the engine torque, Q_E , is related to the rotor speed, Ω , by the following,

$$\dot{\Omega} = (Q_E - Q_R - G_{TR} Q_{TR}) / I_{TR} + \dot{r} \quad (A1.1)$$

where Q_R and Q_{TR} are the main and tail rotor torque's respectively, G_{TR} the tail rotor gear ratio, I_{TR} is the sum of the main rotor, tail rotor, and transmission polar moments of inertia, and \dot{r} , the yaw component of angular acceleration.

The engine torque is automatically controlled by a governing system that relates changes in rotor speed, $\Delta\Omega$, to changes in fuel flow, Δw_f . This part of the governing system is specified in terms of a simple first order lag with gain K_{e1} and time constant τ_{e1} . Its transfer function has the form,

$$\frac{\Delta w_f}{\Delta\Omega} = \frac{K_{e1}}{1 + \tau_{e1} s} \quad (A1.2)$$

The increment in fuel flow change and rotor speed are given by,

$$\Delta w_f = w_f - w_{f_{IDLE}}$$

and,

$$\Delta\Omega = \Omega - \Omega_{IDLE}$$

where $w_{f_{IDLE}}$ and Ω_{IDLE} are the fuel flow and main rotor speed at flight idle. The second part of the governing system relates the changes in fuel flow to changes in engine torque, ΔQ_E and has the form,

$$\frac{\Delta Q_E}{\Delta w_f} = K_{e2} \left(\frac{1 + \tau_{e2} s}{1 + \tau_{e3} s} \right) \quad (A1.3)$$

where,

K_{e2} is the gain associated with the engine response to fuel flow.

ΔQ_E the change in rotor torque from flight idle ($\Delta Q_E = Q_E - Q_{E_IDLE}$).

Q_{E_IDLE} is the rotor torque at flight idle and assumed to have the value $Q_{E_IDLE} = 0$.

τ_{e2} and τ_{e3} are time constants which are functions of engine torque and are given by,

$$\tau_{e2} = \tau_{e20} + \tau_{e21} \left(\frac{Q_E}{Q_{E_MAX}} \right)$$

$$\tau_{e3} = \tau_{e30} + \tau_{e31} \left(\frac{Q_E}{Q_{E_MAX}} \right)$$

where Q_{E_MAX} is the maximum allowable engine torque output.

Combining equations (A1.2) and (A1.3) gives the equations of motion of a power plant and for a single engine system can be shown to be of the form (with some manipulation),

$$\ddot{Q}_E = \frac{1}{(\tau_{e1} \tau_{e3})} \left(-(\tau_{e1} + \tau_{e3}) \dot{Q}_E - Q_E + K_3 (\Omega - \Omega_{IDLE} + \tau_{e2} \dot{\Omega}) \right) \quad (A1.4)$$

where,

$$K_3 = K_{e1} K_{e2}$$

Equations (A1.1) and (A1.4) represent a single engine free turbine power plant. This model has no provision for limiting the torque available from the engine and consequently whatever torque is demanded by the rotors is supplied by the engine via the governor. An example of the response of this model to a step input in engine torque demand is shown in Figure 18. The integration of equations (A1.1) and (A1.4) was achieved by use of a fourth order Runge-Kutta scheme. Initially the torque demand is 5kNm, and after one second, torque required from the engine is increased to 10kNm. It should be noted that the maximum available torque output, Q_{E_MAX} in this case was specified to be 7.5kNm.

To modify the existing engine model for the twin engine case, the first step is to rewrite equation (A1.1) as,

$$\dot{\Omega} = (Q_{E1} + Q_{E2} - Q_R - G_{TR} Q_{TR}) / I_{TR} + \dot{i} \quad (A1.5)$$

where Q_{E1} and Q_{E2} denote the contributions of engine torque output from both engine one and two respectively. The function of varying fuel flow in response to changes in rotor speed in the engine governor is modelled by equation (A1.2). A reasonable assumption is that each engine of a twin gas turbine powerplant will consume fuel at half the rate of an equivalent single engine plant and therefore,

$$K_{e1(i)} = \frac{1}{2} K_{e1} \quad i=1,2$$

Furthermore, the fuel flow module will supply fuel at a sufficient rate to allow any torque demanded to be supplied by the engines and this is demonstrated by Figure 18. In a real gas turbine engine, there is only a finite power output available (usually specified by the manufacturer, although in helicopters maximum available torque is usually limited by the main rotor gearbox). The limiting of the torque produced by each engine is achieved by setting a limit on the fuel flow rate that the engine governing system can deliver. First, write equation (A1.2) as,

$$\frac{\Delta w_{f(i)}^*}{\Delta \Omega^*} = \frac{1}{1 + \tau_{e1} s} \quad (A1.6a)$$

or alternatively,

$$\Delta \dot{w}_{f(i)}^* = \frac{-(\Delta w_{f(i)}^* - \Delta \Omega^*)}{\tau_{e1}} \quad (A1.6b)$$

where,

$$\Delta w_{f(i)}^* = \frac{\Delta w_{f(i)}}{K_{e1(i)}} \quad (A1.6c)$$

and $\Delta \Omega^*$ represents the difference in rotor speed is defined according to the fuel flow schedule. The construction and implementation of the fuel schedule is discussed later in this section.

Now rewrite equation (A1.2) for the multiple engine case and substitute equation (A1.6c) to give,

$$\frac{\Delta Q_{E(i)}}{\Delta w_{f(i)}^*} = K_{3(i)} \left(\frac{1 + \tau_{e2(i)} s}{1 + \tau_{e3(i)} s} \right) \quad (A1.7)$$

where the time constants $\tau_{e2(i)}$ and $\tau_{e3(i)}$ are given by,

$$\tau_{e2(i)} = \tau_{e20} + \tau_{e21} \left(\frac{Q_{E(i)}}{Q_{E \text{ LIM}}} \right)$$

$$\tau_{e3(i)} = \tau_{e30} + \tau_{e31} \left(\frac{Q_{E(i)}}{Q_{E \text{ LIM}}} \right)$$

and,

$$K_{3(i)} = K_{e1(i)} K_{e2}$$

$$Q_{E \text{ LIM}} = \frac{1}{2} Q_{E \text{ MAX}}$$

Manipulation of equation (A1.7) and remembering $Q_{E \text{ IDLE}} = 0$, yields,

$$\dot{Q}_{E(i)} = \frac{1}{\tau_{e3(i)}} \left(K_{3(i)} (\Delta w_{f^* (i)} + \tau_{e2(i)} \Delta \dot{w}_{f^* (i)}) - Q_{E(i)} \right) \quad (\text{A1.8})$$

With respect to the fuel schedule, it is assumed to be a function of the difference in actual and flight idle rotor speed, $\Delta\Omega$. At the condition of maximum torque output from the gas turbine, the fuel flow to the engine will be at a maximum constant level. Furthermore the rotor speed will have dropped below a certain minimum level denoted by, $\Omega_{Q \text{ MAX}}$, giving $\Delta\Omega^* = \Delta\Omega_{\text{MIN}}$ where,

$$\Delta\Omega_{\text{MIN}} = \Omega_{Q \text{ MAX}} - \Omega_{\text{IDLE}} \quad (\text{A1.9})$$

so that $\Delta\Omega_{\text{MIN}}$ is naturally a negative quantity. During normal engine torque output operating limits, the fuel schedule is given by,

$$\Delta\Omega^* = \Delta\Omega$$

When rotor speed is greater than the maximum rotor speed, the fuel flow is shut off (so that its value cannot be negative) by setting $\Delta\Omega^*$ to zero. Hence the three operating conditions of the fuel schedule can be written as,

$$\Delta\Omega^* = \begin{cases} \Delta\Omega_{\text{MIN}} & \Delta\Omega_{\text{MIN}} \geq \Delta\Omega \\ \Delta\Omega & 0 < \Delta\Omega < \Delta\Omega_{\text{MIN}} \\ 0 & \Delta\Omega \geq 0 \end{cases}$$

The variation of fuel flow, Δw_f^* (i), with rotor speed, $\Delta\Omega^*$, is shown graphically in Figure 19.

In constructing the fuel schedule, it is necessary to evaluate the minimum rotor speed at which maximum engine torque output is achieved, Ω_{QMAX} .

Let,

$$\Omega_{\text{QMAX}} = \Omega_{\text{IDLE}} \gamma \quad (\text{A1.10})$$

where γ denotes a rotor droop factor. Substituting equation (A1.10) into (A1.9) and rearranging for γ gives,

$$\gamma = \frac{\Delta\Omega_{\text{MIN}}}{\Omega_{\text{IDLE}}} + 1 \quad (\text{A1.11})$$

Under steady conditions equation (A3.4) reduces to,

$$Q_E = K_3 \Delta\Omega \quad (\text{A1.12})$$

If the power plant is at maximum steady output, then equation (A1.12) can be written as,

$$Q_{E \text{ MAX}} = K_3 \Delta\Omega_{\text{MIN}}$$

and substituting this expression into equation (A1.11) enables the rotor droop factor to be evaluated from,

$$\gamma = \frac{Q_{E \text{ MAX}}}{K_3 \Omega_{\text{IDLE}}} + 1$$

Therefore equations (A1.5), (A1.6b) and (A1.8) represent a twin gas turbine powerplant with a limited power output. An example of the use of this model is shown in Figure 3. In this

test case, both engines are initially generating 5kNm torque to met a demand of 10kNm. The maximum available torque from each gas turbine is specified to be 7.5kNm. At $t=0.5s$, number two engine is failed and subsequently engine number one begins to increase its torque output to compensate for the reduced net torque output. With the torque required from the powerplant held at 10kNm, it can be seen that the engine governor never permits this torque demand to be met by the remaining engine.

Appendix 2.

A2. Mathematical Model of an Artificial Stability and Flight Control System

A mathematical model of an artificial stability and flight control system will now be presented. Each of the collective, longitudinal and lateral cyclic control channels will be discussed in turn.

i) Collective Channel

The pilot contribution to collective pitch, θ_{op} , is given by,

$$\theta_{op} = g_{co} + g_{c1} \eta_c$$

where g_{co} , g_{c1} are gearing constants and η_c is the collective lever position ($0 \leq \eta_c \leq 1$). The gearing constants are derived from the swashplate upper and lower collective limits. The autostab contribution to collective swashplate angle, θ_{oa} , is obtained from a normal accelerometer so that,

$$\theta_{oa} = k_g \Delta n$$

where,

$$\Delta n = 1 + \frac{a_z}{g}$$

and,

k_g is the accelerometer feedback gain ,
 a_z is the normal body axis acceleration,
 g is the acceleration due to gravity.

The net displacements from the pilot and autostab are passed through a hydraulic actuator modelled as a first order lag, so that its transfer function has the form,

$$\frac{\theta_o}{\theta_{op} + \theta_{oa}} = \frac{1}{1 + \tau_{c4} s}$$

where,

τ_{c4} is a time constant,

θ_o is the combined collective displacement after actuation

ii) Longitudinal Cyclic Channel

The longitudinal cyclic displacement at the swashplate is function of both the pilot longitudinal cyclic and collective lever inputs and effectively limits blade pitch angles in forward flight. A nonlinear gearing map is used to link the two controls in the actual aircraft, although a linearised version of the map is prescribed in the mathematical model.

Due to rotor cross - coupling effects (not discussed here for brevity), a pure forward cyclic stick displacement in rotor that rotates anticlockwise when viewed from above for example, will not only cause the rotor disc to pitch forward, but it will also result in a rolling motion to the right. To help counteract this, the longitudinal and lateral cyclic displacements are mixed or 'phased' after actuation in manner governed by the following equations,

$$\theta_{1s} = \theta_{1s}^* \cos \psi_f + \theta_{1c}^* \sin \psi_f$$

$$\theta_{1c} = \theta_{1c}^* \cos \psi_f - \theta_{1s}^* \sin \psi_f$$

where,

θ_{1s} , θ_{1c} are the longitudinal and lateral cyclic displacements at the swashplate after mixing ,

θ_{1s}^* , θ_{1c}^* are the longitudinal and lateral cyclic stick displacements prior to mixing,

ψ_f is the cyclic mixing angle .

The operation of the phasing is best described by example. A forward pitching movement of the rotor disc requires θ_{1s}^* to be negative, however cyclic cross coupling effects will result in an additional rolling of the rotor disc to the right. Recalling positive displacements of θ_{1c}^* give a roll to the left and since θ_{1s}^* is negative, an opposing left rolling moment is generated as indicated by equation (A4.1).

For the flight control system, the pilot contribution to longitudinal cyclic displacement prior to mixing, θ_{1sp}^* , can be given by,

$$\theta_{1sp}^* = g_{1s0} + g_{1s1} \eta_{1s} + (g_{sc0} + g_{sc1} \eta_{1s}) \eta_c$$

where,

g_{1s0} , g_{1s1} are gearing constants associated with the longitudinal cyclic,

g_{sc0} , g_{sc1} are gearing constants associated with the collective contribution,

η_{1s} is the pilot longitudinal cyclic stick position ($0 \leq \eta_{1s} \leq 1$).

The autostabiliser contribution to longitudinal cyclic, θ_{1sa}^* , is obtained from the proportional and derivative action feedback of the pitch attitude, θ , and pitch rate, q . An additional feed forward term based on pilot stick position with respect to some datum is also included. Thus the longitudinal autostabiliser contribution can be obtained from,

$$\theta_{1sa}^* = k_{\theta} \theta + k_q q + k_{1s} (\eta_{1s} - \eta_{1s0})$$

where,

k_{θ} is a proportional action feedback gain,

k_q is a derivative action feedback gain,

k_{1c} is the feed forward gain,

η_{1s0} is the reference pilot stick position, ($0 \leq \eta_{1s0} \leq 1$).

As in the collective case, the combined autostabiliser and pilot contributions to longitudinal cyclic are passed through a hydraulic actuator which in this mathematical model is represented as a first order lag. The transfer function is then given by,

$$\frac{\theta_{1s}^*}{\theta_{1sp}^* + \theta_{1sa}^*} = \frac{1}{1 + \tau_{c1} s}$$

where τ_{c1} is the time constant associated with the longitudinal actuator.

iii) Lateral Cyclic Channel

The lateral cyclic displacement at the swashplate due to pilot inputs, θ_{1c}^* , is a function of cyclic stick movements only and is given by,

$$\theta_{1c}^* = g_{1c0} + g_{1c1} \eta_{1c}$$

where,

g_{1c0} , g_{1c1} are stick gearing constants,

η_{1c} is the pilot lateral cyclic stick displacement ($0 \leq \eta_{1c} \leq 1$).

The autostabiliser contribution to the lateral cyclic channel is derived from the proportional and derivative action feedback of roll attitude, ϕ , and roll rate, p , respectively. An additional feed forward term based on lateral stick position with respect to some datum

value is also included. Thus the lateral cyclic contribution from the autostab, $\theta_{1c_a}^*$, can be given by,

$$\theta_{1c_a}^* = k_\phi \phi + k_p p + k_{1c} (\eta_{1c} - \eta_{1c0})$$

where,

k_ϕ is a proportional action feedback gain,

k_p is a derivative action feedback gain,

k_{1c} is the feed forward gain,

η_{1c0} is the reference pilot stick position, ($0 \leq \eta_{1c0} \leq 1$).

The transfer function of the combined pilot and autostab contributions is given as,

$$\frac{\theta_{1c}^*}{\theta_{1c_p}^* + \theta_{1c_a}^*} = \frac{1}{1 + \tau_{c2} s}$$

where τ_{c2} the time constant of the actuator.

iv) Yaw Channel

The pilot contribution to tailrotor swashplate displacement is made up from signals from both the collective lever and pedal. A linear relationship is used to combine the collective and pedal inputs into an equivalent term known as cable length, η_{ct} . The cable length is expressed in the following manner,

$$\eta_{ct} = g_{ct0} (1 - \eta_p) + (1 - 2 g_{ct0}) \eta_c$$

where,

g_{ct0} is the gearing constant used in the combination of collective lever and pedal displacements,

η_p is the pilot pedal displacement, ($0 \leq \eta_p \leq 1$).

The pilot contribution to tailrotor collective, θ_{otp} , can then be given by,

$$\theta_{otp} = g_{t0} + g_{t1} \eta_{ct}$$

where g_{t0} and g_{t1} gearing constants.

The autostabiliser contribution to the yaw channel, θ_{ota} , is obtained from proportional and derivative action feed back of the heading, ψ , and yaw rate, r . A 'heading - hold' facility is also included. The autostab contribution can be written as,

$$\theta_{ota} = k_{\psi} (\psi - \psi_H) + k_r r$$

where,

k_{ψ} , k_r is the proportional and derivative action feed back respectively,
 ψ_H is the heading hold term that is adjustable by the pilot.

The transfer function of the combined pilot and autostab contributions to the tailrotor collective displacement is given as,

$$\frac{\theta_{ot}}{\theta_{otp} + \theta_{ota}} = \frac{1}{1 + \tau_{c3} s}$$

where τ_{c3} the time constant of the actuator.

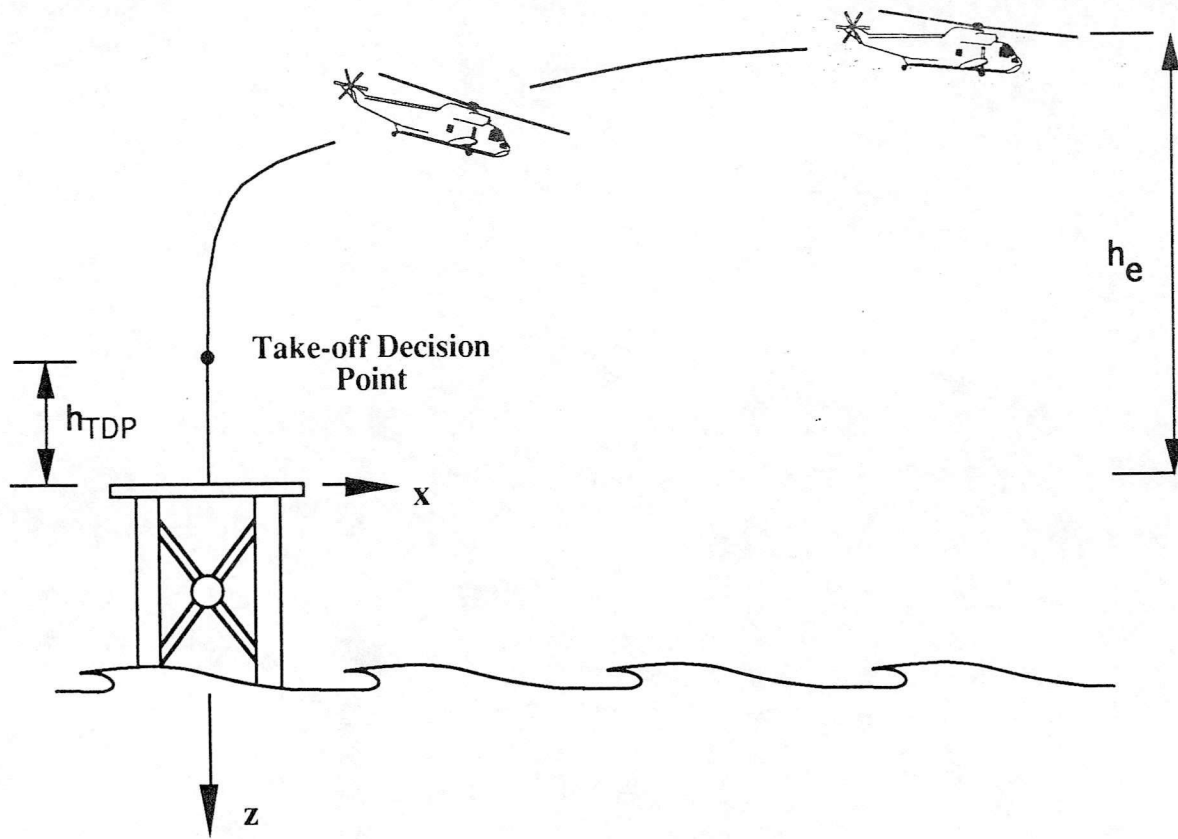
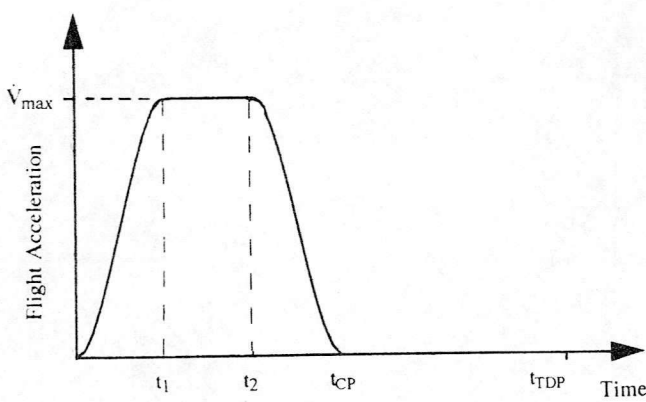
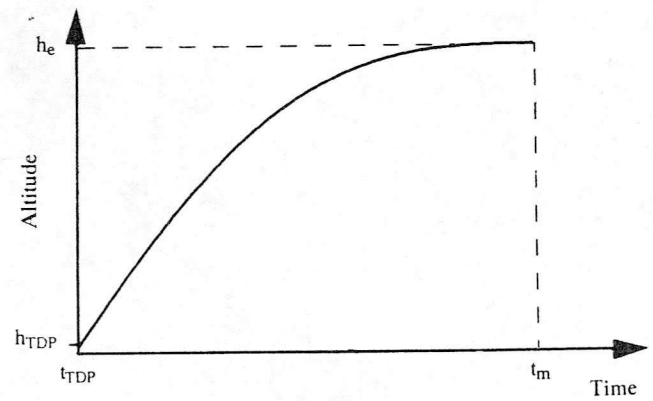


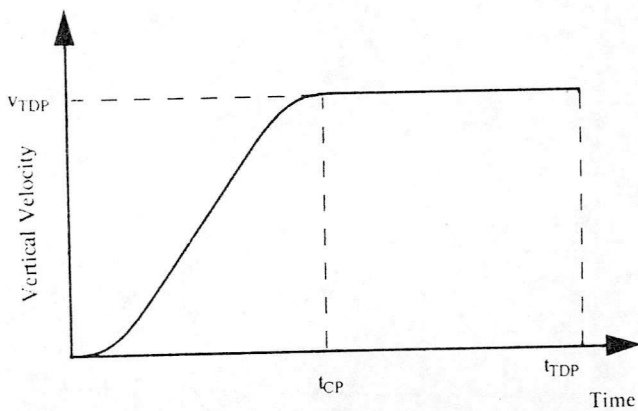
Figure 1 : Towering Takeoff Manoeuvre



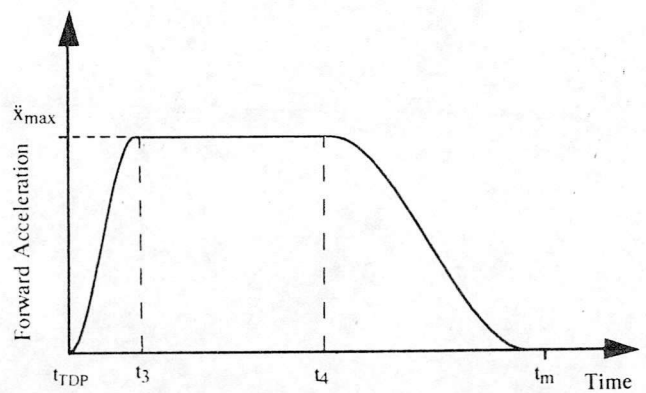
a) Flight Acceleration



c) Altitude



b) Vertical Velocity



d) Forward Acceleration

Figure 2 : Flight Path Parameters For Towering Takeoff Manoeuvre

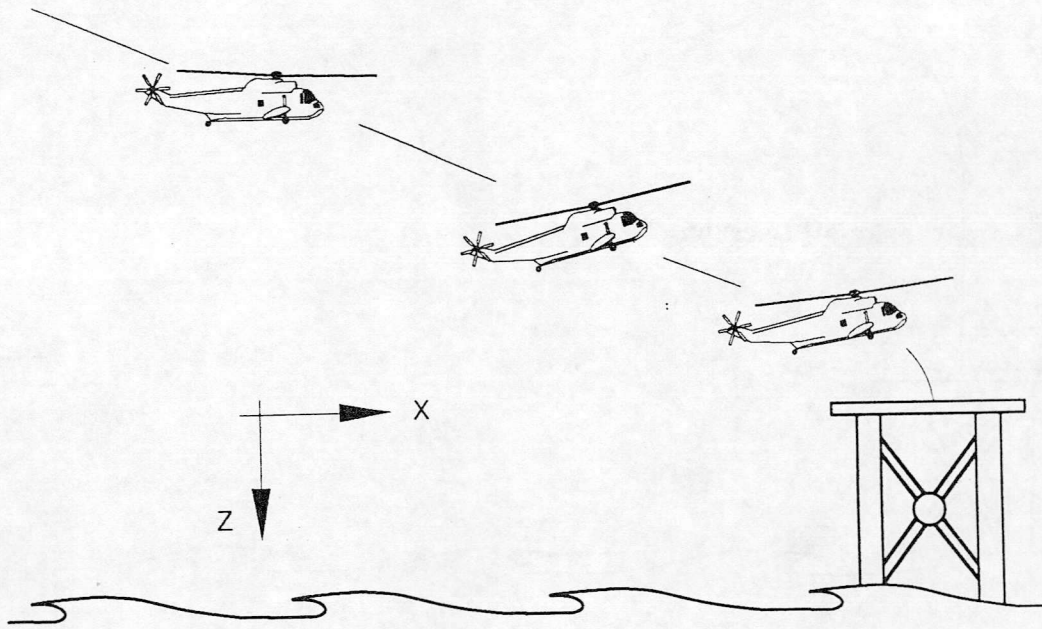


Figure 3 : Normal Approach and Landing Manoeuvre

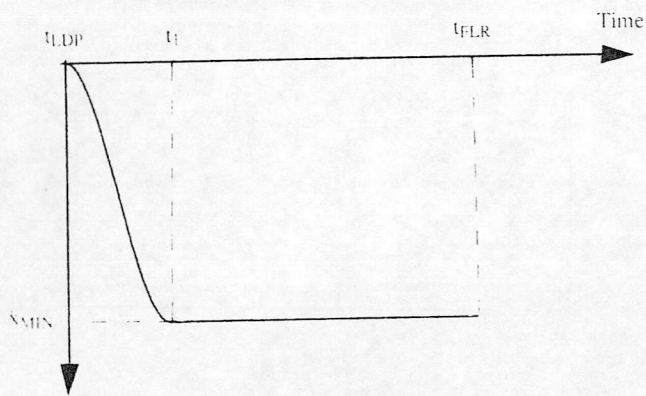


Figure 4a : Flight Acceleration

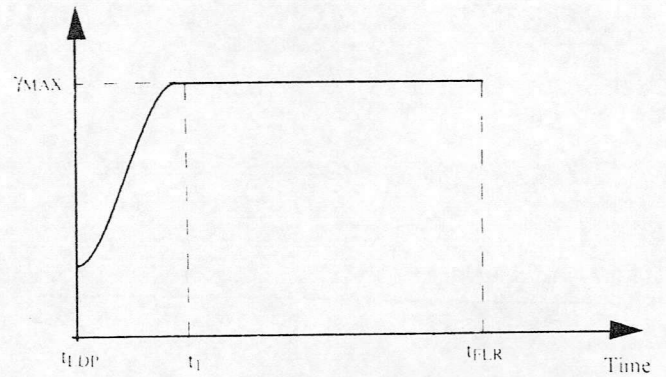


Figure 4b : Descent Angle

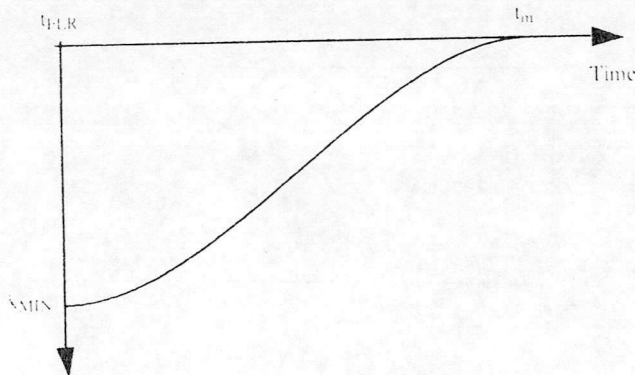


Figure 4c : Forward Acceleration

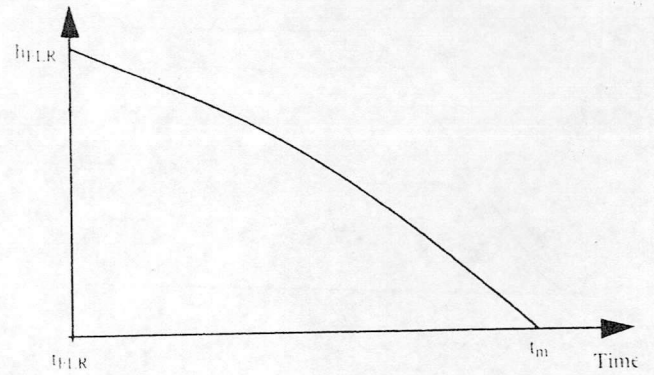


Figure 4d : Altitude

Figure 4 : Flight Path Parameters for Normal Approach and Landing

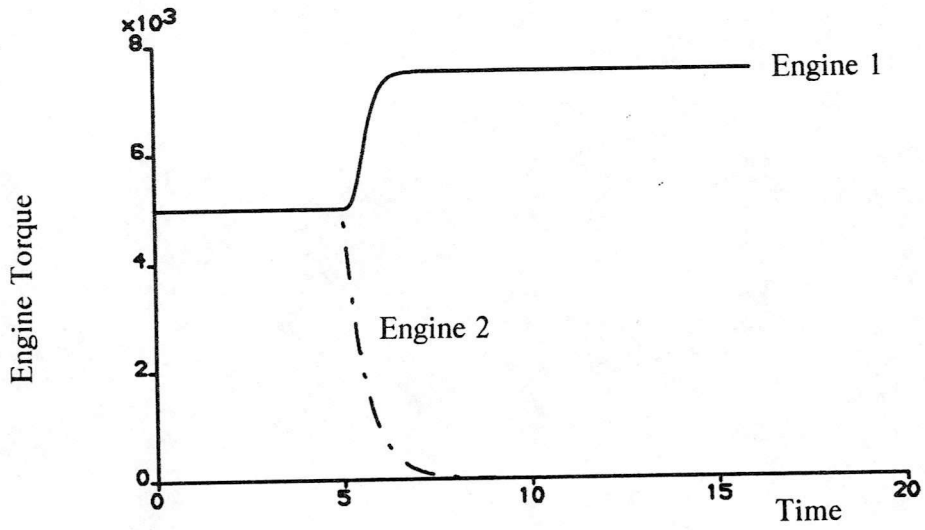


Figure 5 : Torque Time History for Engine Failure

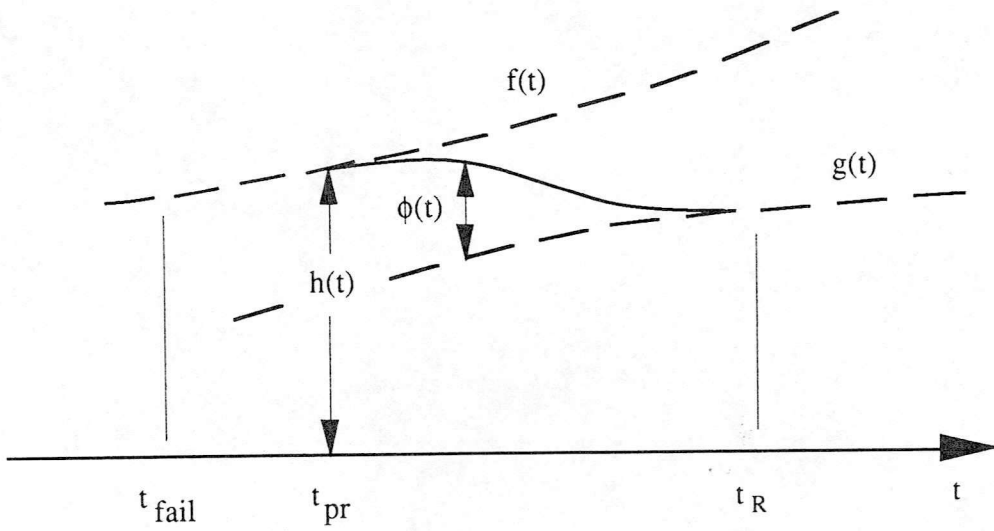


Figure 6 : Blending Function for Recovery Flight Path

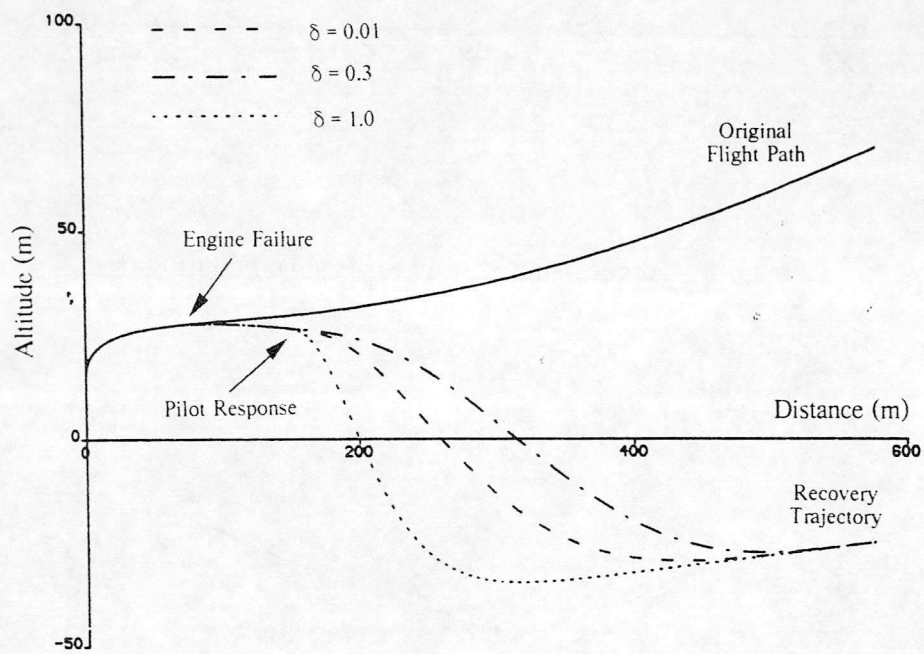


Figure 7 : Effect of Value of δ on Recovery Trajectory

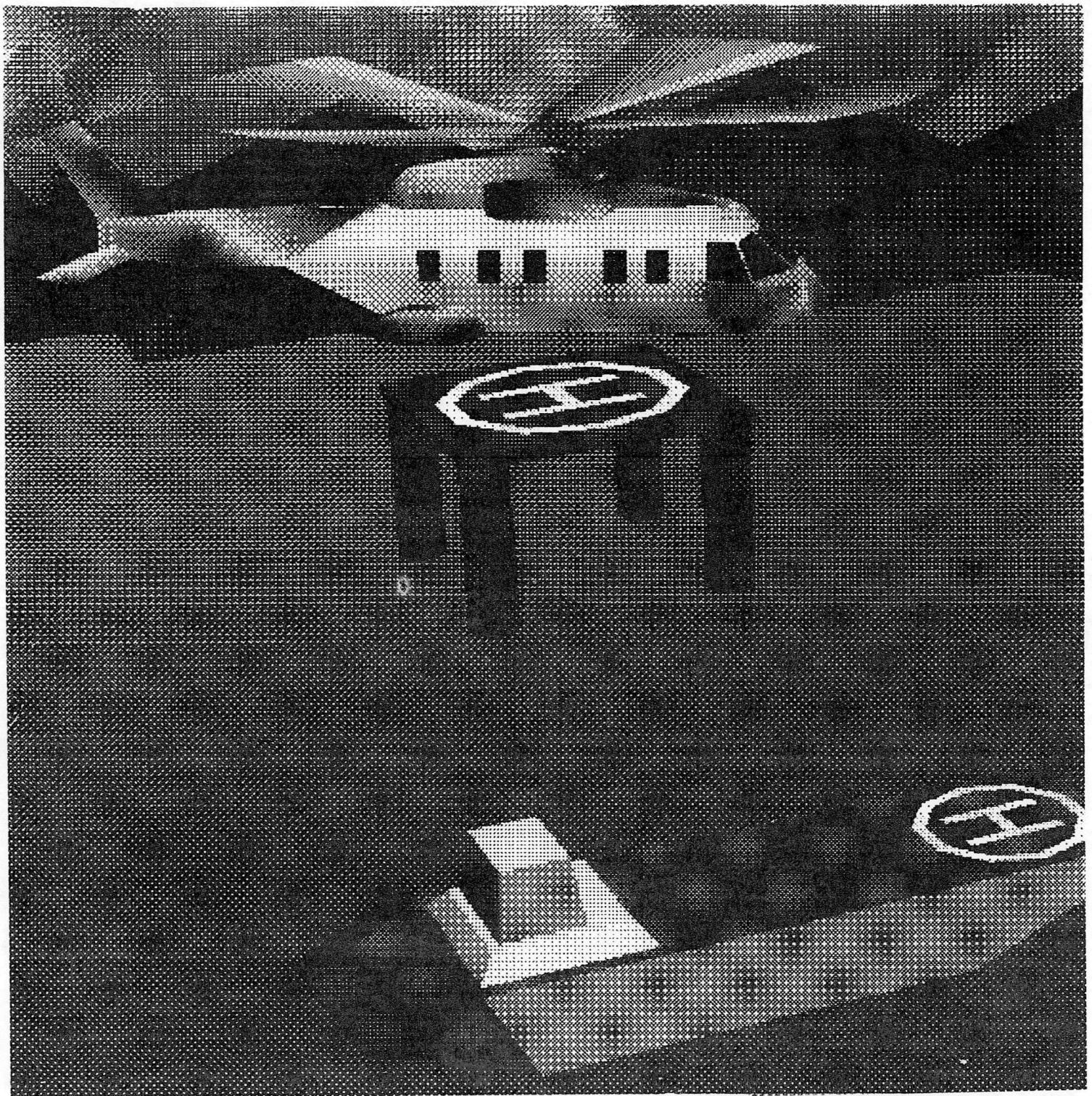


Figure 8 : Hogs Enviroment

Figure 9 : Towering Takeoff Flight Paths

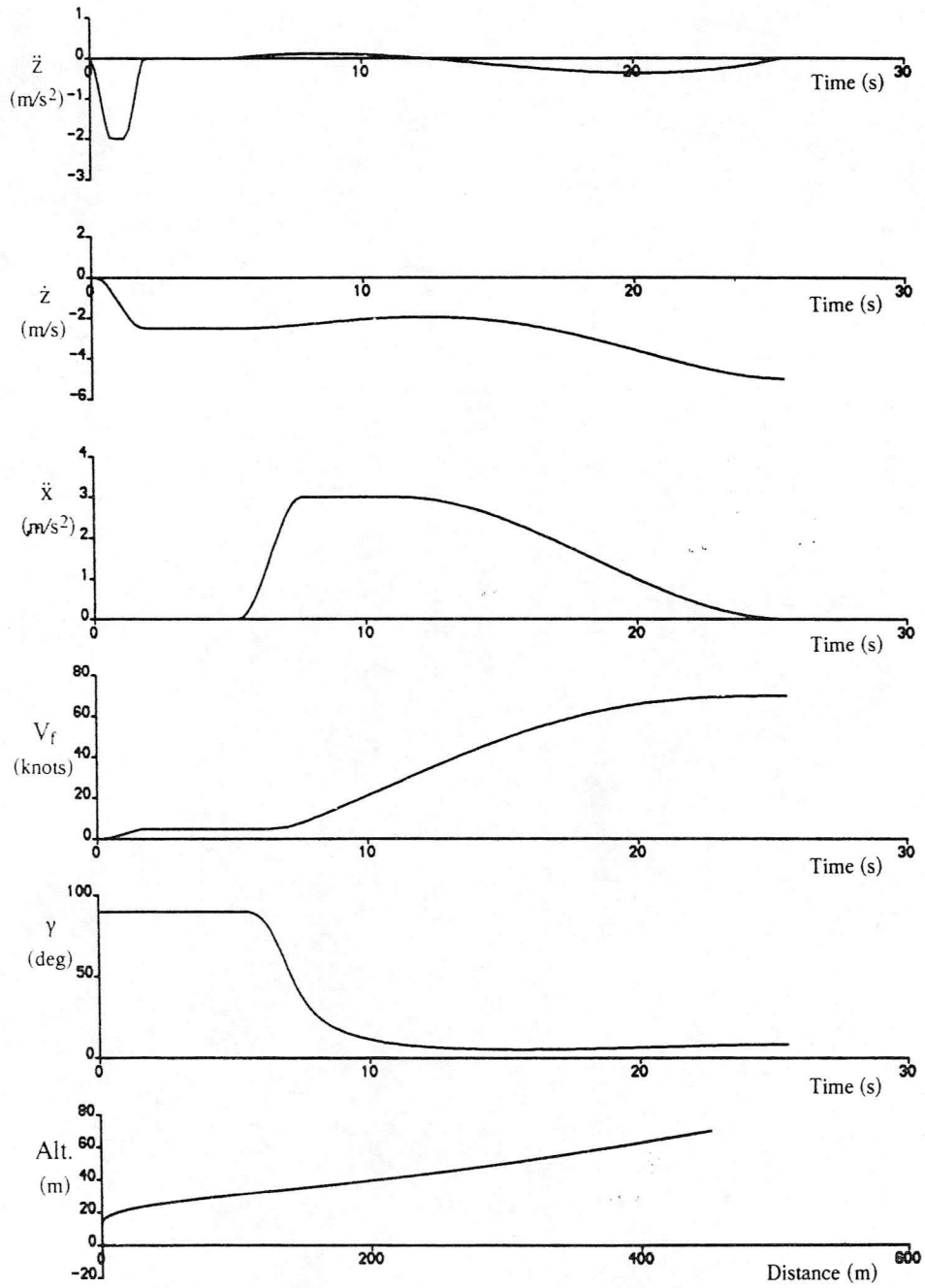


Figure 10 : Inverse Simulation of Towering Takeoff

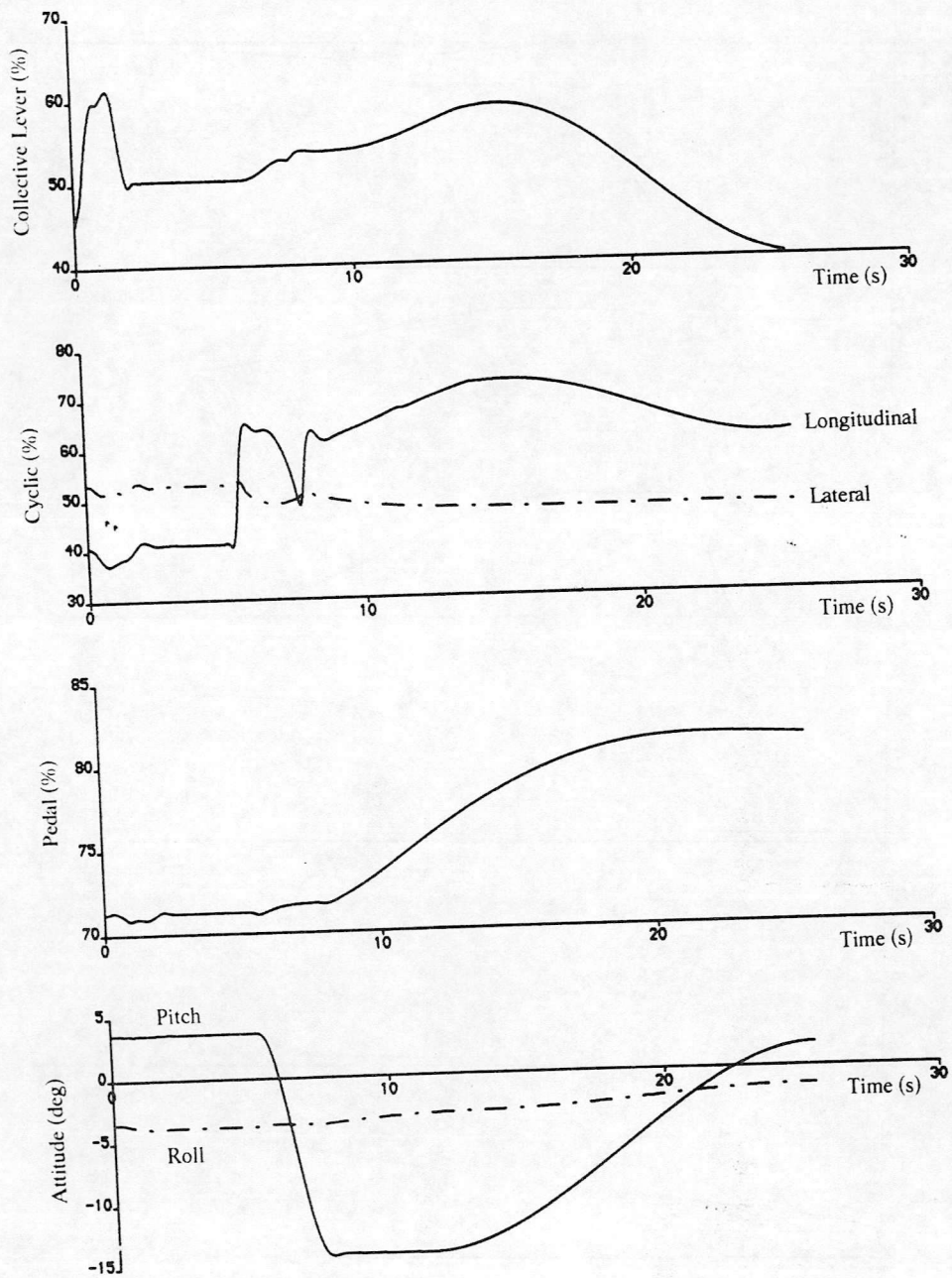


Figure 10 (Continued) : Inverse Simulation of Towering Takeoff

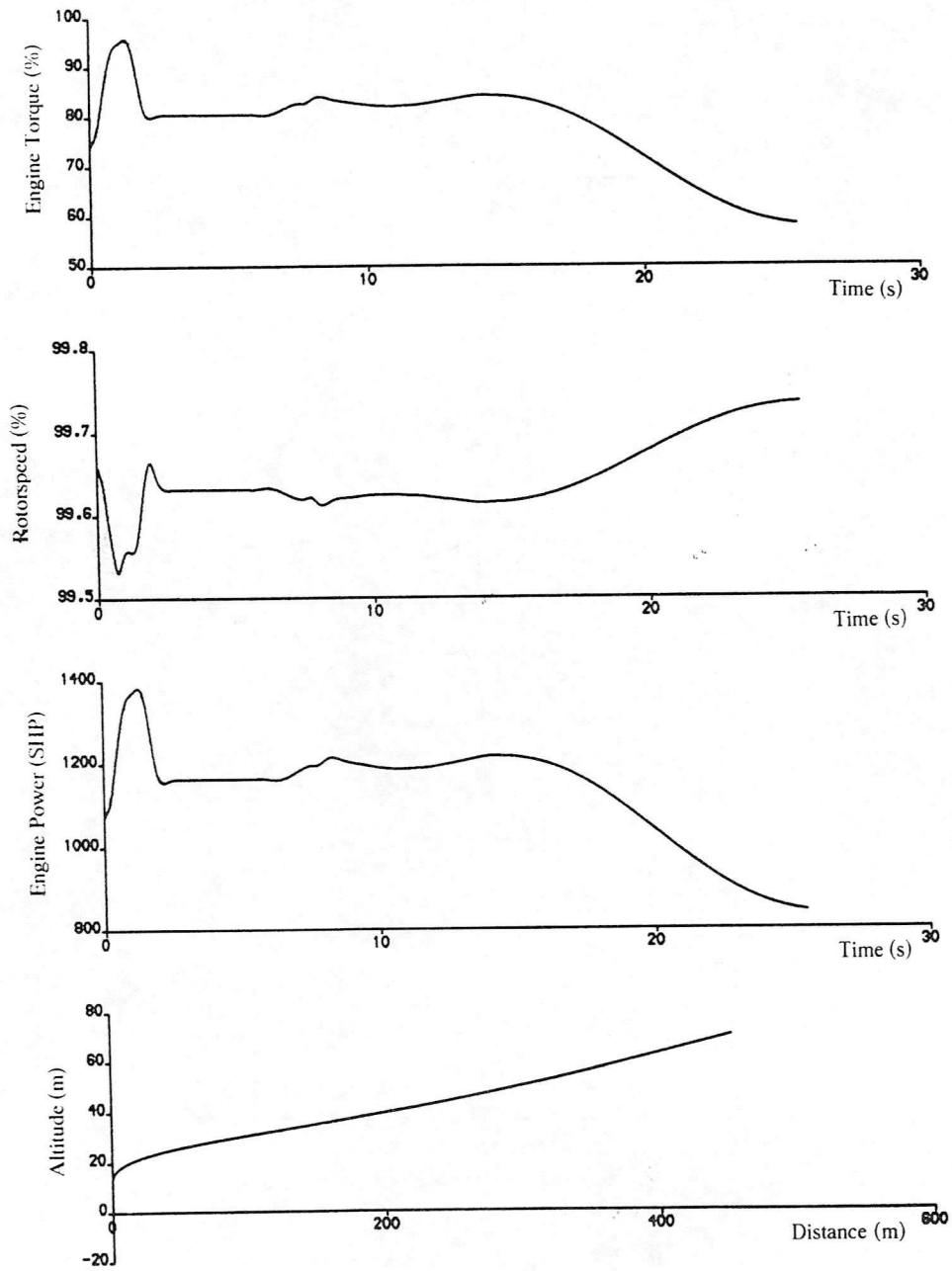


Figure 11 : Inverse Simulation of Towering Takeoff with Engine Failure Prior to TDP

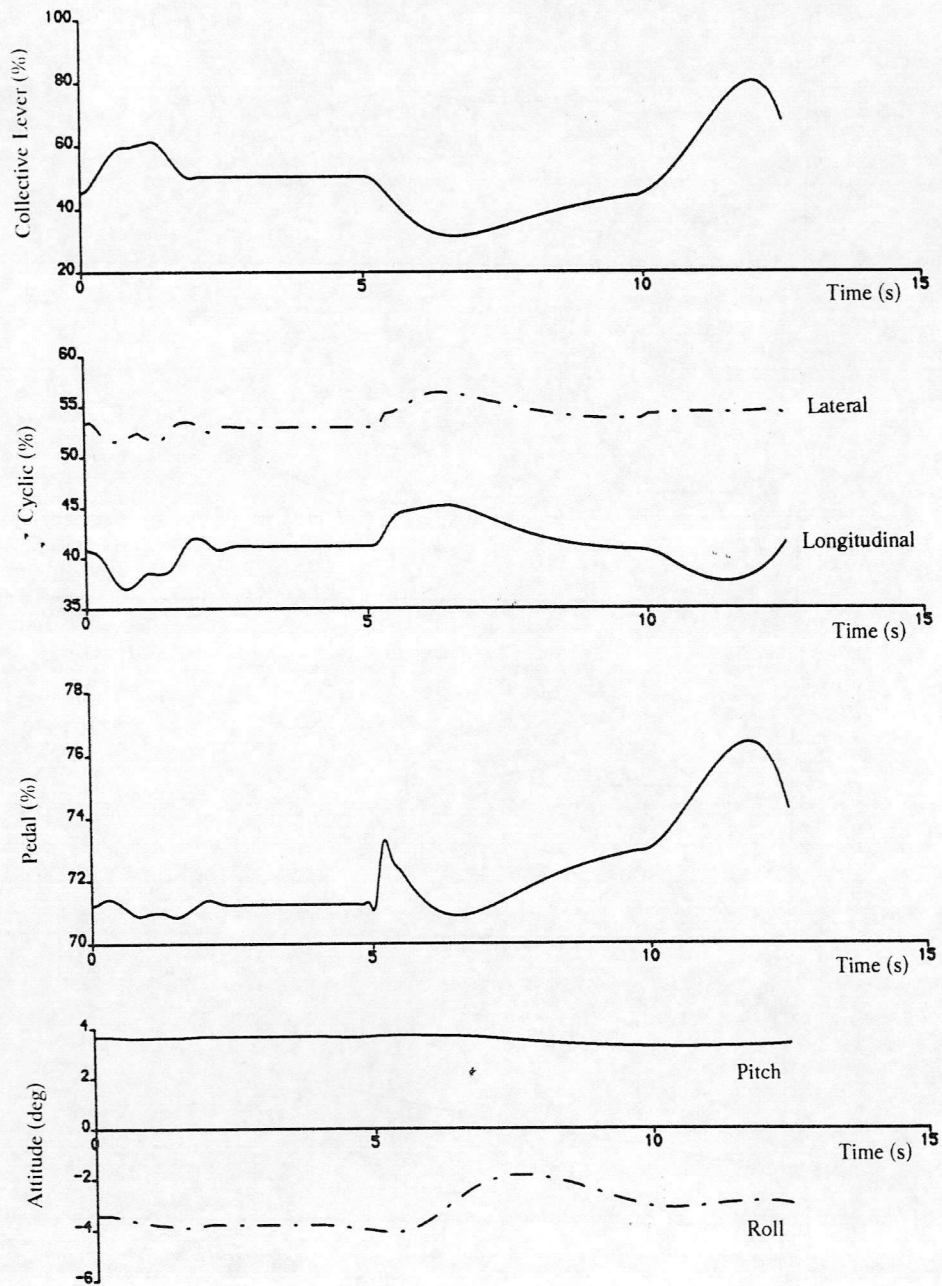


Figure 11 (Continued) : Inverse Simulation of Towering Takeoff with Engine Failure Prior to TDP

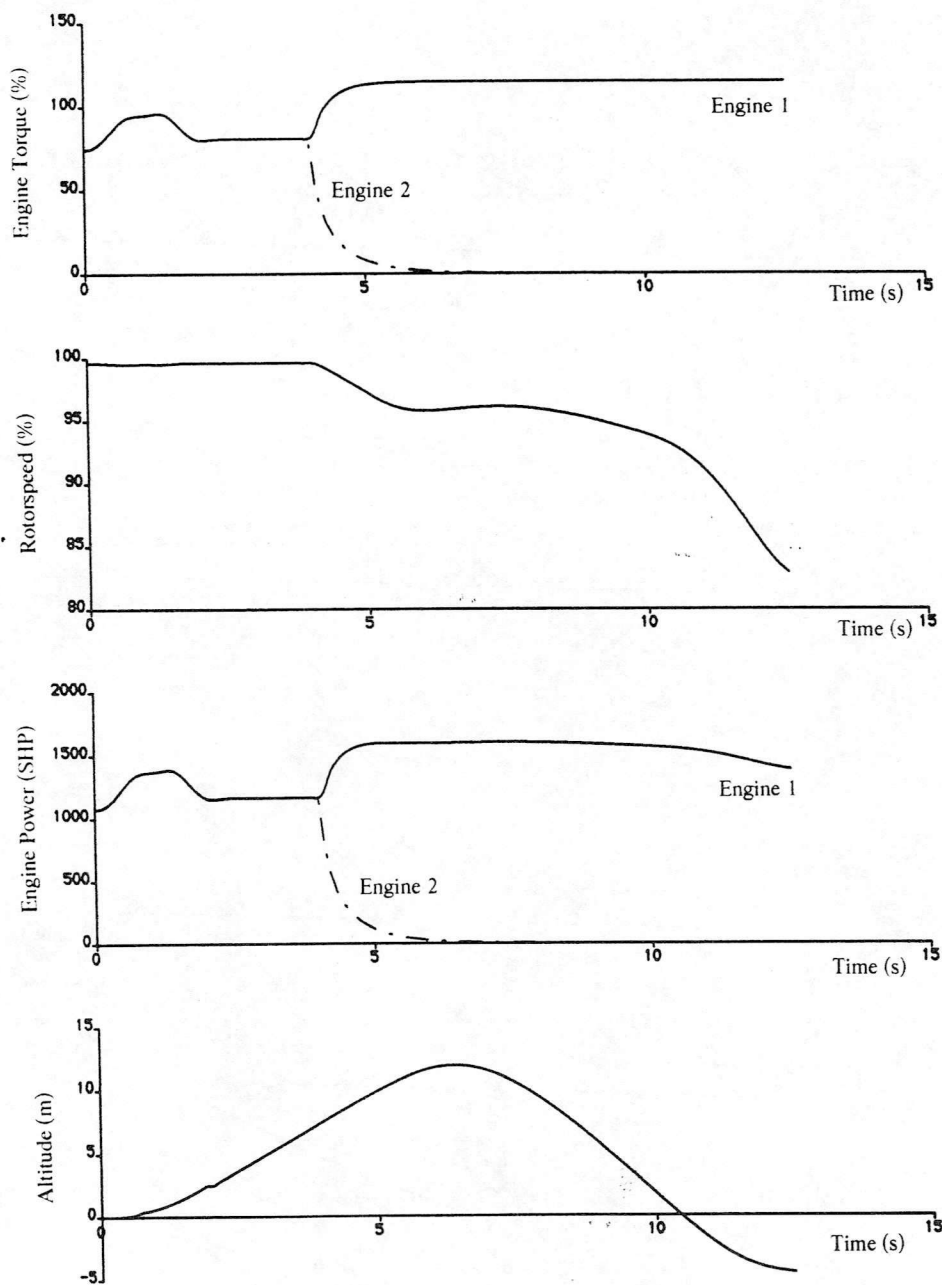


Figure 12 : Inverse Simulation of Towering Takeoff with Engine Failure Just After TDP

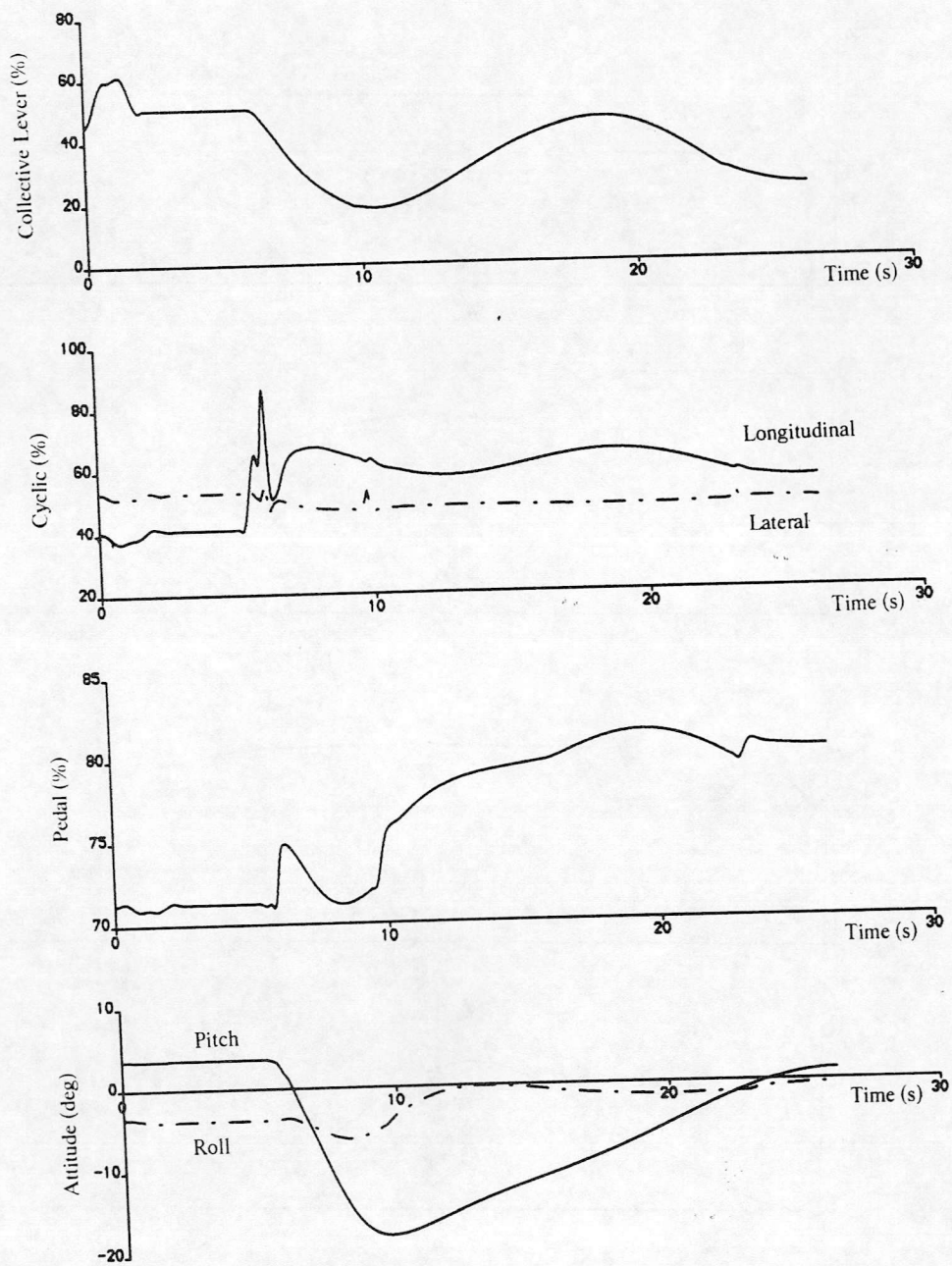


Figure 12 (Continued) : Inverse Simulation of Towering Takeoff with Engine Failure Just After TDP

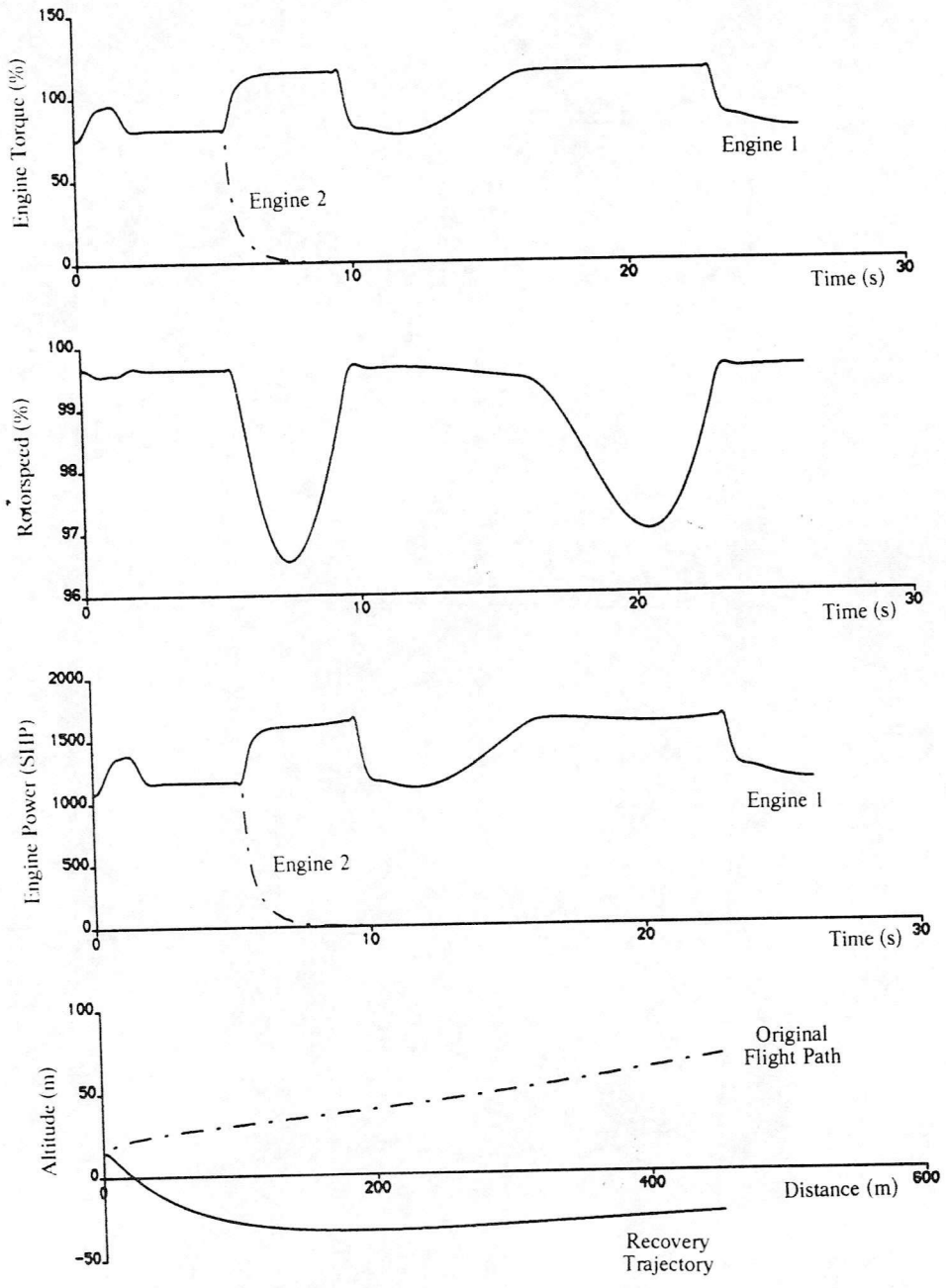


Figure 13 : Inverse Simulation of Towering Takeoff with Engine Failure Well After TDP

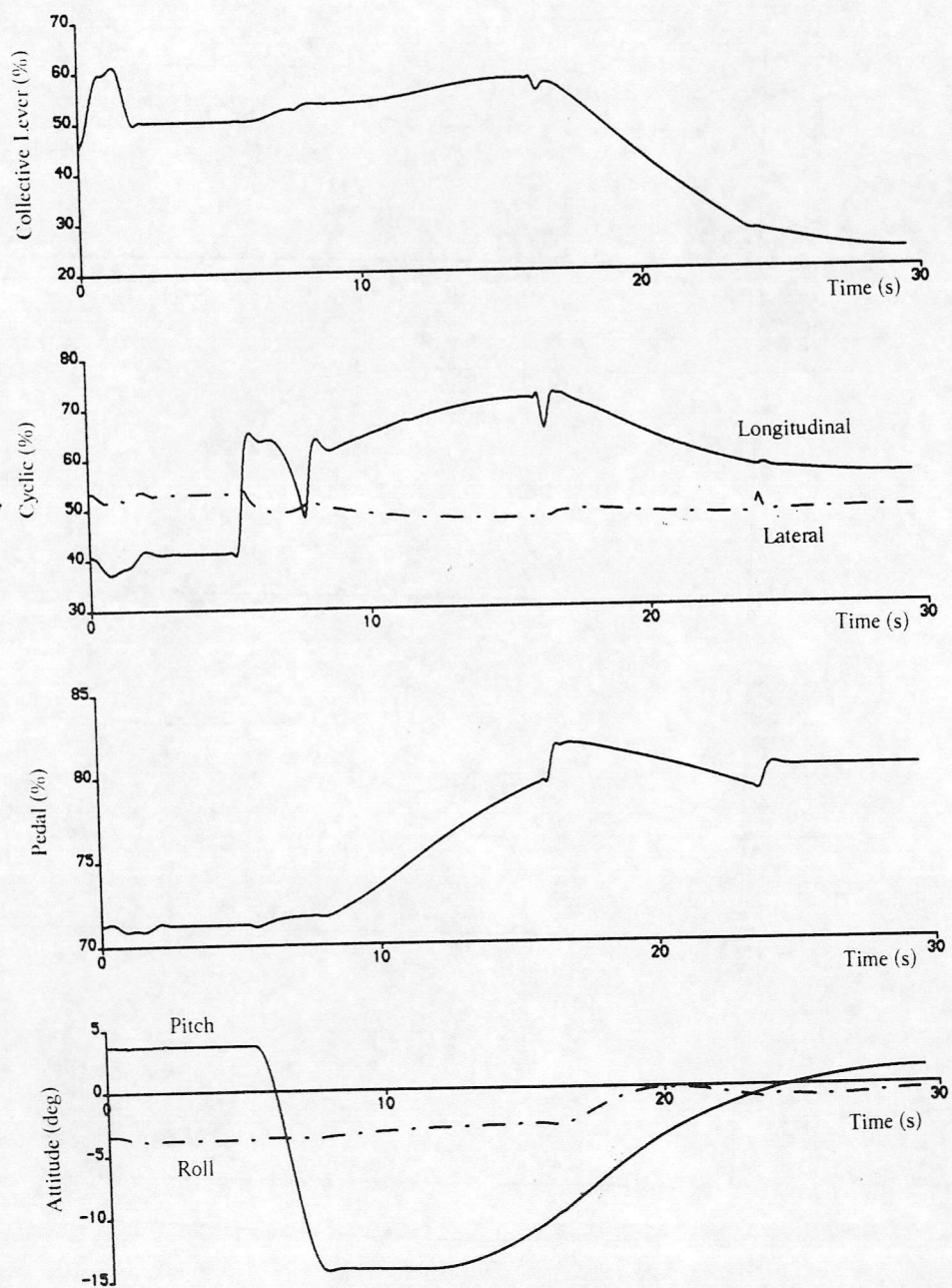


Figure 13 (Continued) : Inverse Simulation of Towering Takeoff with Engine Failure Well After TDP

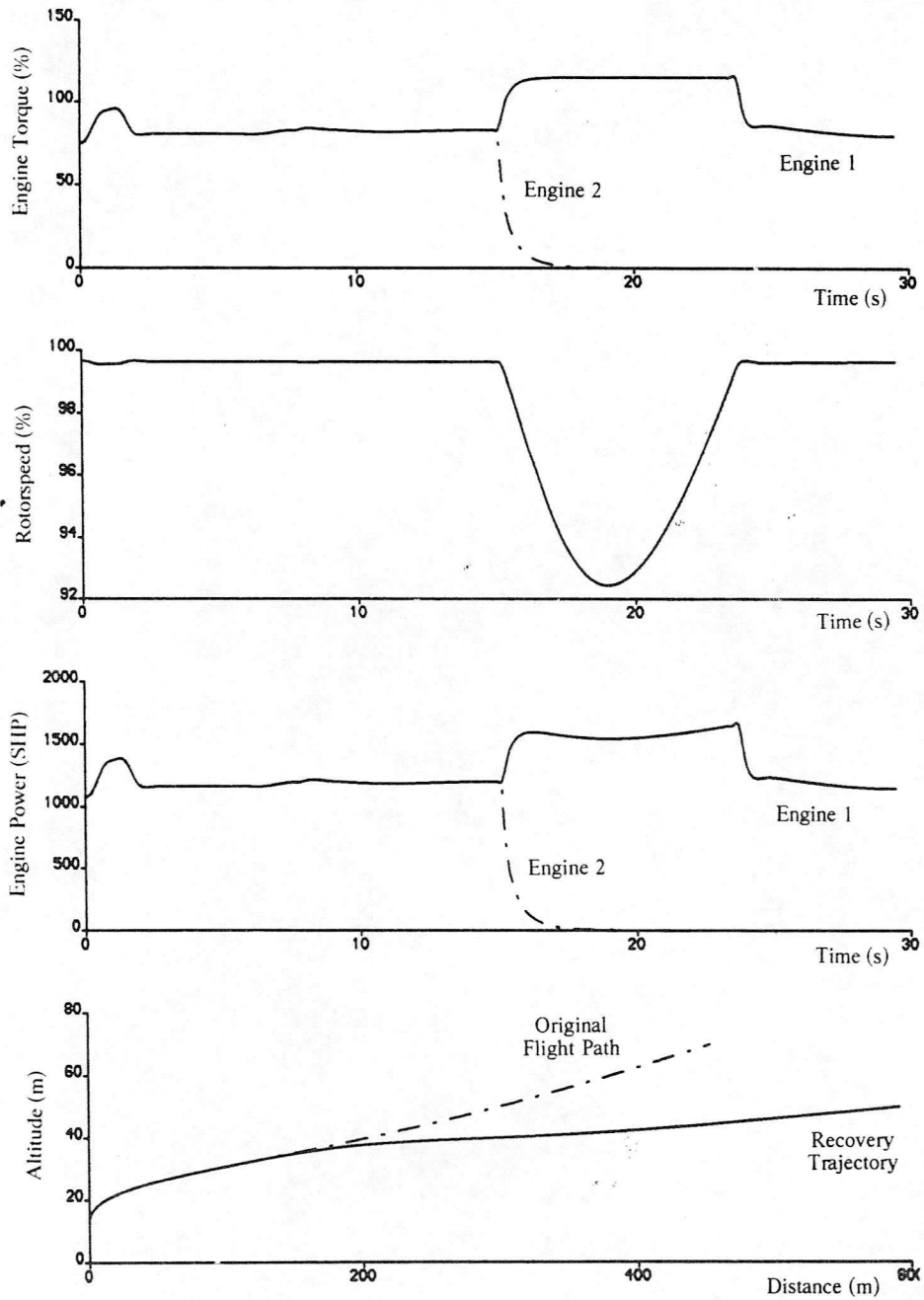


Figure 14 : Normal Approach and Landing Flight Paths

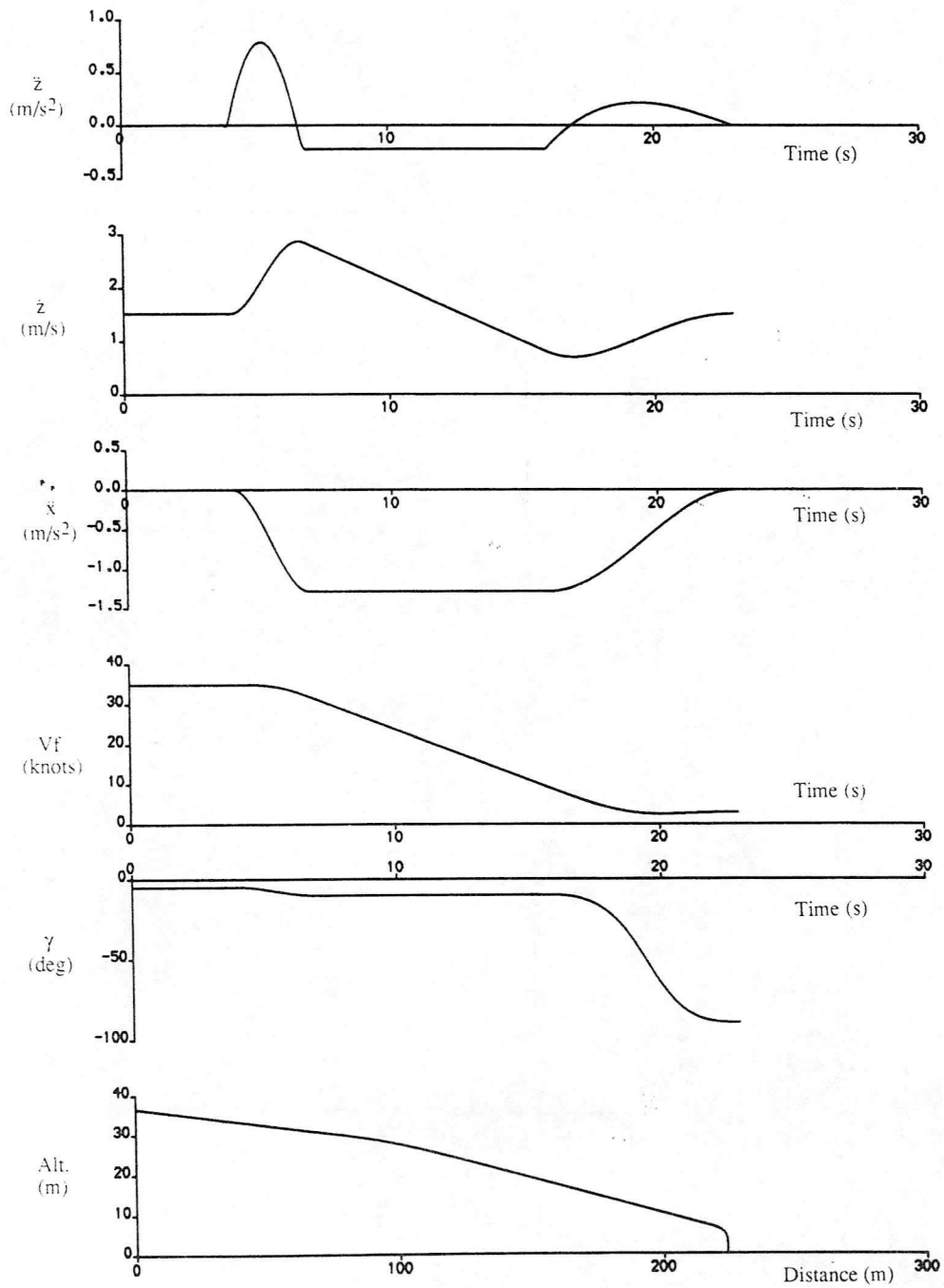


Figure 15 : Inverse Simulation of Normal Approach and Landing

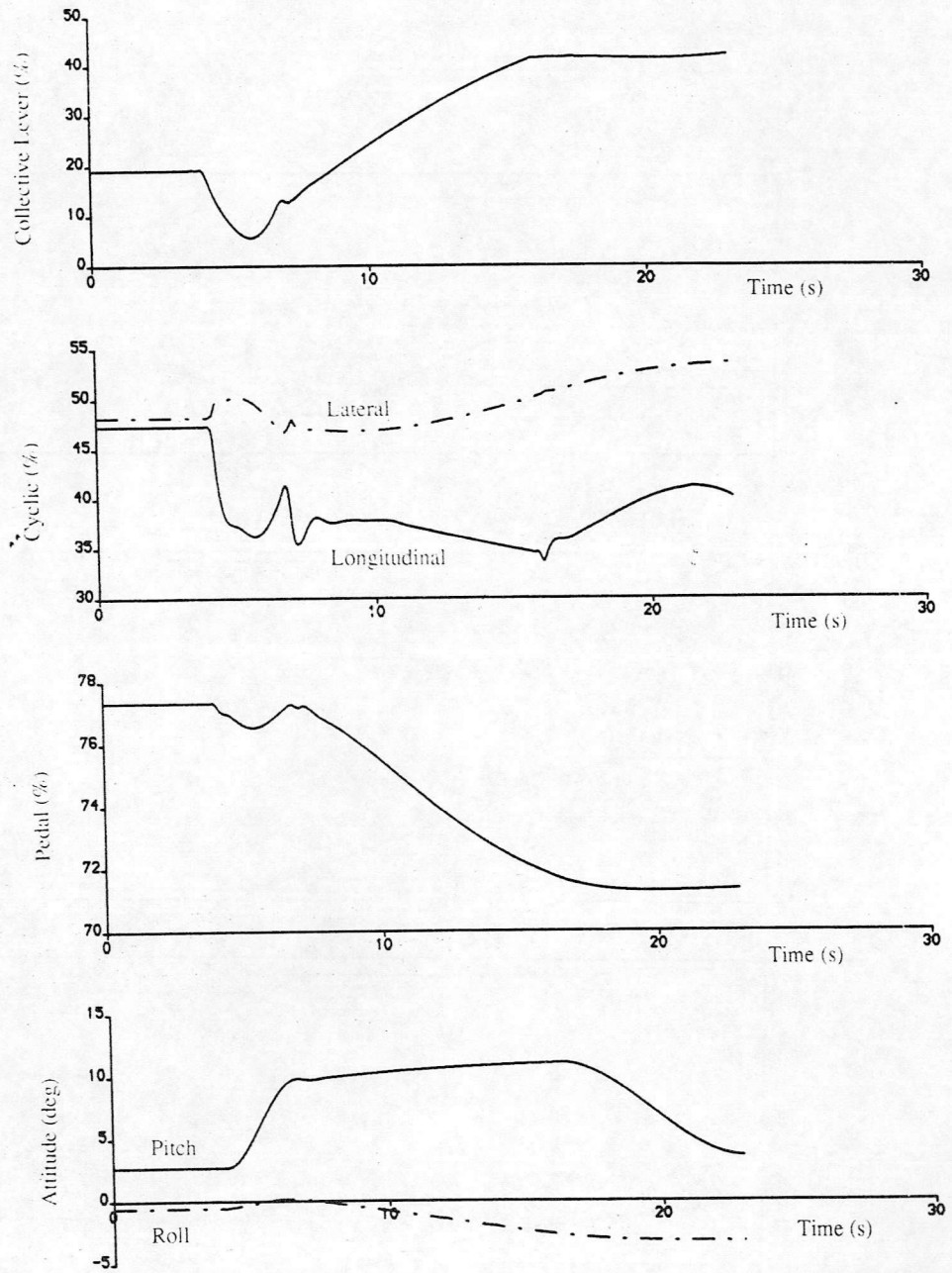


Figure 15 (Continued) : Inverse Simulation of Normal Approach and Landing

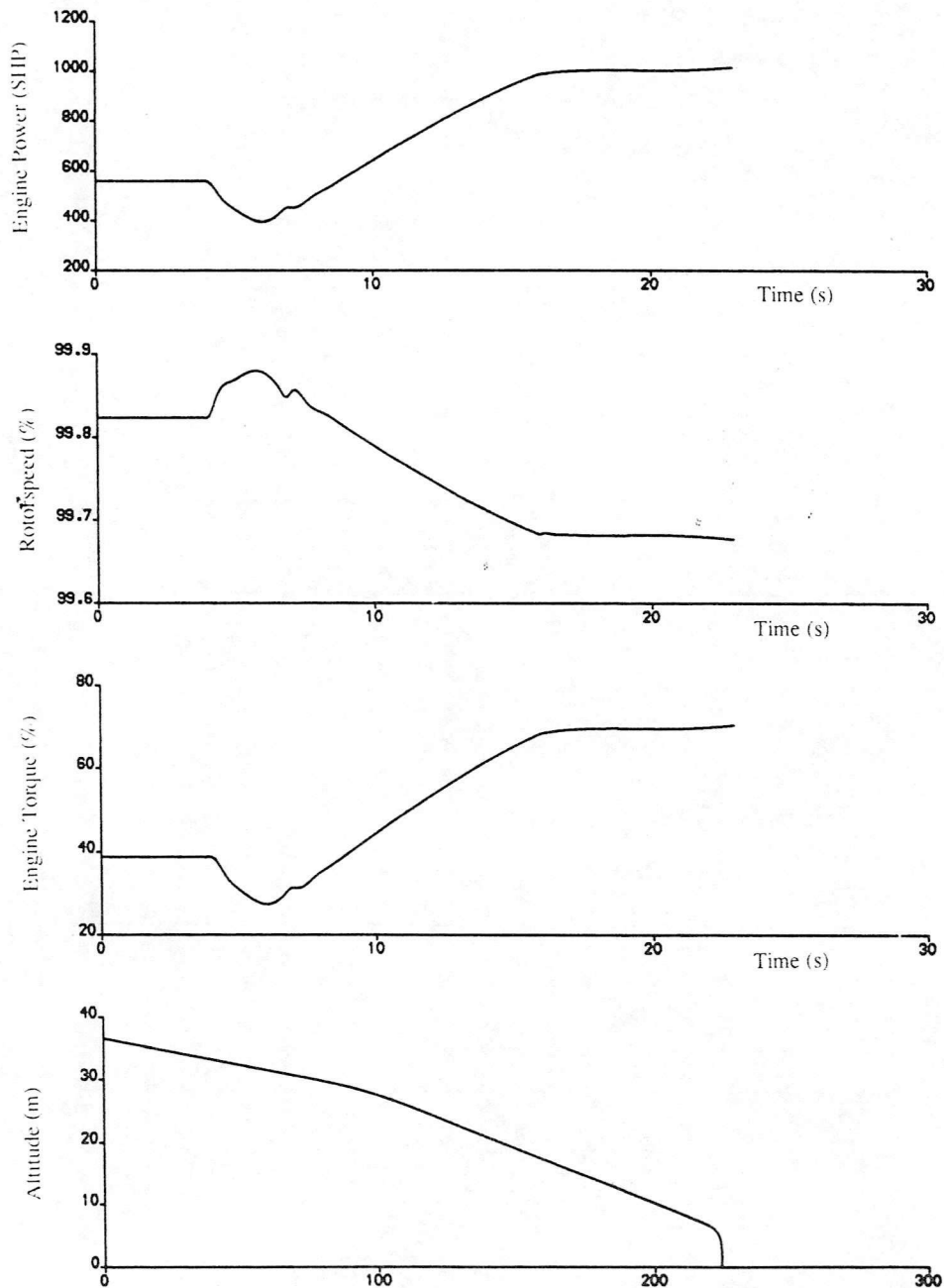


Figure 16 : Inverse Simulation of Normal Approach and Landing with Engine Failure Prior to LDP

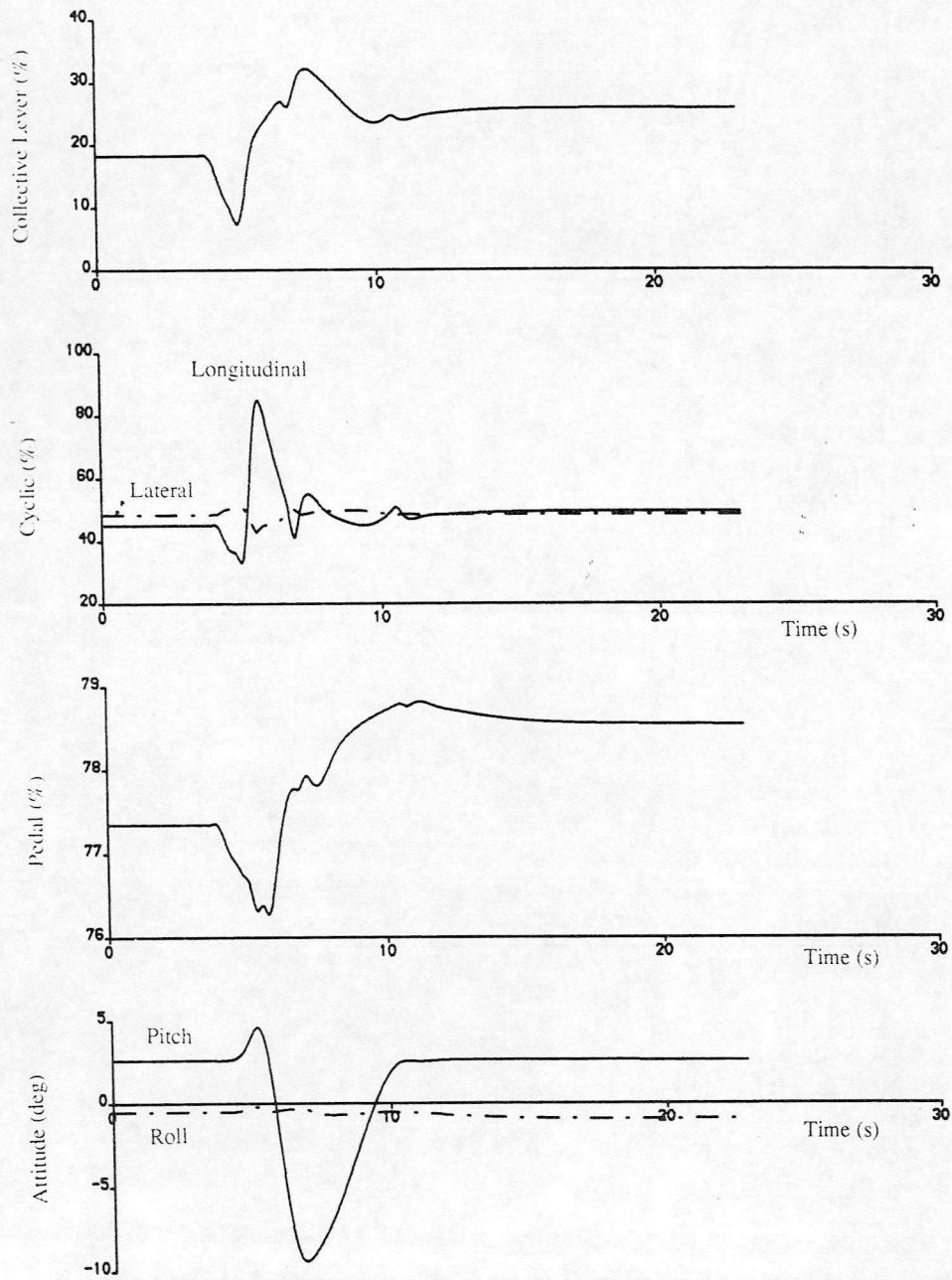


Figure 16 (Continued) : Inverse Simulation of Normal Approach and Landing with Engine Failure Prior to LDP

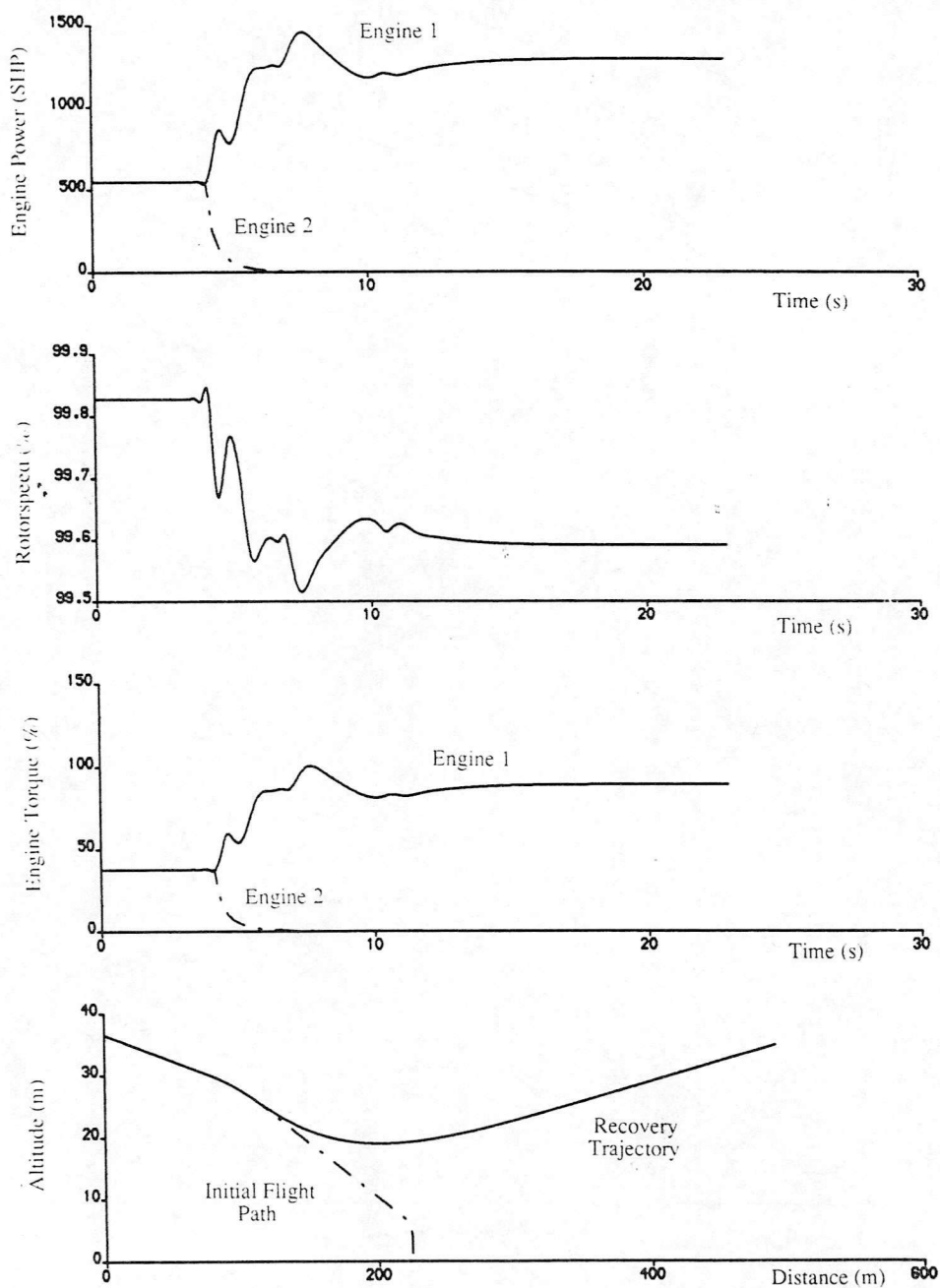


Figure 17 : Inverse Simulation of Normal Approach and Landing with Engine Failure Just After TDP

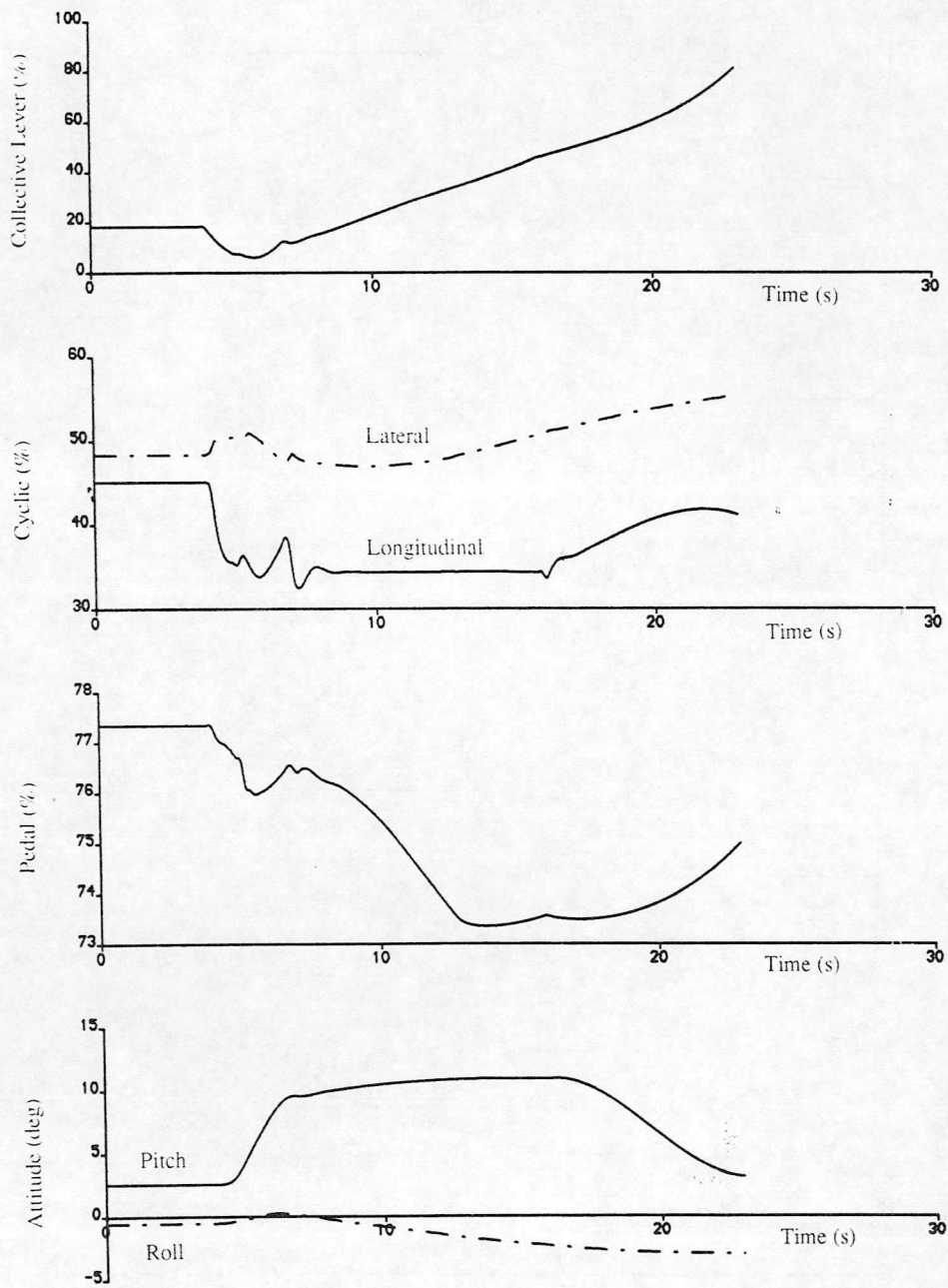
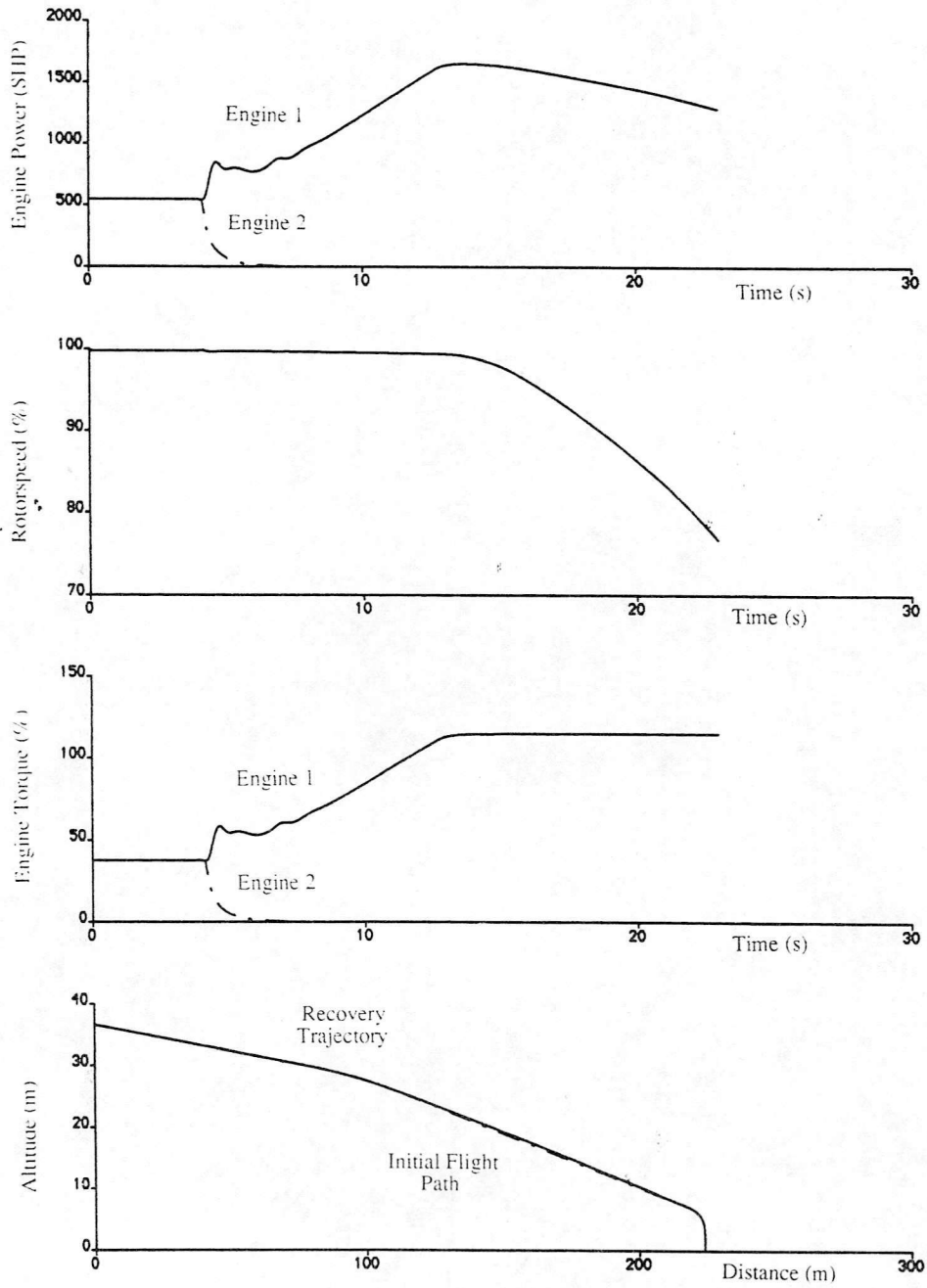


Figure 17 (Continued) : Inverse Simulation of Normal Approach and Landing with Engine Failure Just After TDP



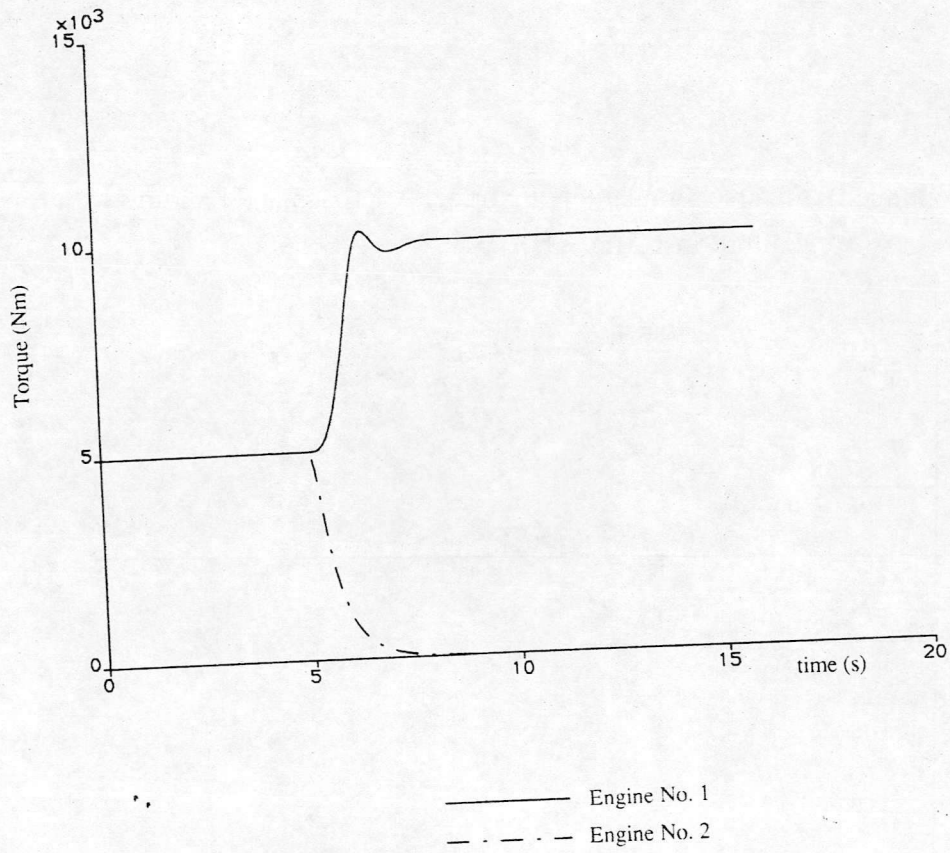


Figure 18 : Unlimited Torque Output Engine Response

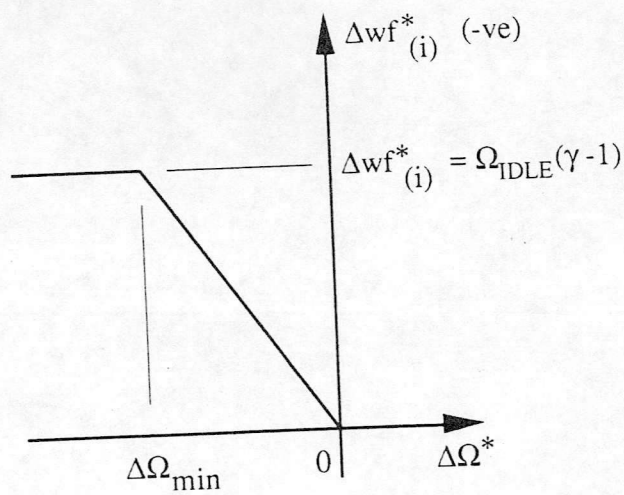


Figure 19: Fuel Flow Schedule

